# GENIALG

## GENetic diversity exploitation for Innovative macro-ALGal biorefinery

## *Deliverable D2.1*

# Biobanking of wild and currently cultivated *Ulva* and *S. latissima* strains with associated genotyping and phenotyping data

**Planned delivery date (as in DoA):** April 2020 - M40

**Actual submission date**: April 2020

**Workpackage:** WP2 - Selection, breeding, germplasm and biobanking

**Workpackage leader**: CNRS (France)

**Deliverable leader:** SAMS (United Kingdom)

**Version:** 1.0

| **Project co-funded by the European Commission within the Horizon 2020 Programme (2014 - 2020)** | |
|---|---|
| **Dissemination Level** | |
| **PU** Public | **PU** |
| **CI** Classified, as referred to Commission Decision 2001/844/EC | |
| **CO** Confidential, only for members of the consortium (including the Commission Services) | |

Start date of the project: January 1st, 2017

This project has received funding from the European Union's Horizon 2020 research and innovation programme under grant agreement No. 727892 (GENIALG). This output reflects only the author's view and the European Union cannot be held responsible for any use that may be made of the information contained therein.

# Biobanking of wild and currently cultivated *Ulva* and *S. latissima* strains with associated genotyping and phenotyping data

Marie-Mathilde PERRINEAU[1], Claire GACHON[1], Cecilia RAD-MENÉNDEZ[1,2], Callum O'CONNELL[1], Carla RUIZ-GONZALEZ[1], Pedro MURÚA[1], Martina STRITTMATTER[1], Yacine BADIS[1], Paola ARCE[1], Elisabete DA COSTA[3,4], Ricardo CALADO[5], Rosário DOMINGUES[3,4], Maria Helena ABREU[6], Bárbara PITARMA[6], Madalena MENDES[6], Adrie VAN DER WERF[7], Annelies BENIERS[7], Antoine FORT[8], Ronan SULPICE[8], Silje FORBORD[9], Jorunn SKJERMO[9], Isabel COSTA AZEVEDO[10], Helena AMARO[10], Rosa MELO[10], Isabel SOUSA-PINTO[10,11], Paulo RUGGERI[12,13], Christophe DESTOMBE[13], Lucie JAUGEON[13], Stéphane MAUGER[13], Myriam VALERO[13], J. Mark COCK[12].

[1] Scottish Association for Marine Science, Scottish Marine Institute, Oban, United Kingdom.
[2] Culture Collection of Algae and Protozoa, Scottish Association for Marine Science, Scottish Marine Institute, Oban, United Kingdom.
[3] Mass Spectrometry Centre, LAQV REQUIMTE, Department of Chemistry, University of Aveiro, Santiago University Campus, 3810-193 Aveiro, Portugal.
[4] CESAM - Centre for Environmental and Marine Studies, Department of Chemistry, University of Aveiro, Santiago University Campus, 3810-193 Aveiro, Portugal.
[5] ECOMARE, CESAM - Centre for Environmental and Marine Studies, Department of Biology, University of Aveiro, Santiago University Campus, 3810-193 Aveiro, Portugal.
[6] ALGAplus, Produção e Comercialização de Algas e seus derivados Lda. PCI-Via do Conhecimento, 3830-352 Ílhavo, Portugal.
[7] Wageningen University & Research, Business unit Agrosystems Research, P.O. Box 16, NL-6700AA Wageningen, The Netherlands.
[8] National University of Ireland - Galway, Plant Systems Biology Lab, Ryan Institute & MaREI Centre for Marine, Climate and Energy, School of Natural Sciences, Galway, H91 TK33, Ireland.
[9] SINTEF Ocean, Department of Environment and New Resources, 7465 Trondheim, Norway.
[10] CIIMAR - Interdisciplinary Centre of Marine and Environmental Research of the University of Porto Novo Edifício do Terminal de Cruzeiros do Porto de Leixões, Avenida General Norton de Matos, S/N 4450-208 Matosinhos, Portugal.
[11] FCUP - Faculty of Sciences of the University of Porto, Rua do Campo Alegre 1021/1055, 4169-007 Porto, Portugal.
[12] CNRS, Sorbonne Université, Algal Genetics Group, UMR 8227, Integrative Biology of Marine Models, Station Biologique de Roscoff, CS 90074, F-29688, Roscoff, France.
[13] CNRS, Sorbonne Université, UC, UACH, Evolutionary Biology and Ecology of Algae, UMI 3614, Station Biologique de Roscoff, CS 90074, F-29688, Roscoff, France.

# Contents

# Figures

# Tables

# Executive summary

This deliverable summarises the collection, genotyping, phenotyping and biobanking of wild and cultivated *S. latissima* and *Ulva* spp. strains (i.e. WP2, Task 1). Wild and industrial strains of both species were **collected** throughout the geographic areas covered by GENIALG. At the time of collection, *S. latissima* and *Ulva* were **phenotyped** for different characteristics of industrial interest such as morphometry, growth, physiological and metabolic parameters (e.g. lipids, polysaccharides, proteins, amino acids...). Additional **high throughput phenotyping** protocols were developed under controlled conditions. Likewise, these two algae have been **genetically** characterized using different techniques (microsatellites markers i.e. SSRs; RAD-seq as SNPs, GWAS or QTL; whole genome sequencing, barcoding, CAPS assay…).
For *Saccharina latissima*, the genetic diversity of 700 wild sporophytes (parental i.e. F0) and their offspring (F1), their morphology and growth phenotypes have been or are being acquired to identify QTLs underpinning traits of agronomic interest (CNRS). Clonal gametophytes have been isolated from the same wild sporophytes. They will be genetically characterised and phenotyped for disease resistance against an oomycete pathogen after the Covid-19 lockdown, to identify QTLs linked to biotic stress responses (SAMS). For *Ulva* spp., the considerable genetic, growth and metabolic differences observed in the panel of more than 200 strains analysed at present indicate a strong potential for strain selection to increase productivity in aquaculture setups (NUIG). Finally, **biobanks** of *S. latissima* and *Ulva* spp. have been established. A **cryopreservation** protocol has been established for *S. latissima* gametophytes and successful preliminary tests of *Ulva* spp. have been conducted as well.

# 1. *Saccharina latissima*

## 1.1. Introduction

### 1.1.1. *S. latissima* life cycle

*Saccharina latissima* has a haplo-diploid life cycle, similar to other cultivated kelp species such as *Saccharina japonica, Undaria pinnatifida* and *Alaria esculenta* (FAO, 2018). Diploid sporophytes produce meiotic sporangia that release haploid zoospores (Figure 1). Once settled, zoospores develop into haploid gametophytes. The species is dioecious, with male or female gametophytes that are microscopic, filamentous and morphologically very different from the diploid, meter-long sporophyte. Upon sexual maturation, gametophytes release gametes; upon syngamy, female eggs are fertilised by male sperm form a zygote which then develops into a diploid sporophyte. Even before their maturation, it is possible to the trained eye to differentiate between male and female gametophytes, a property that has been particularly useful in this work.

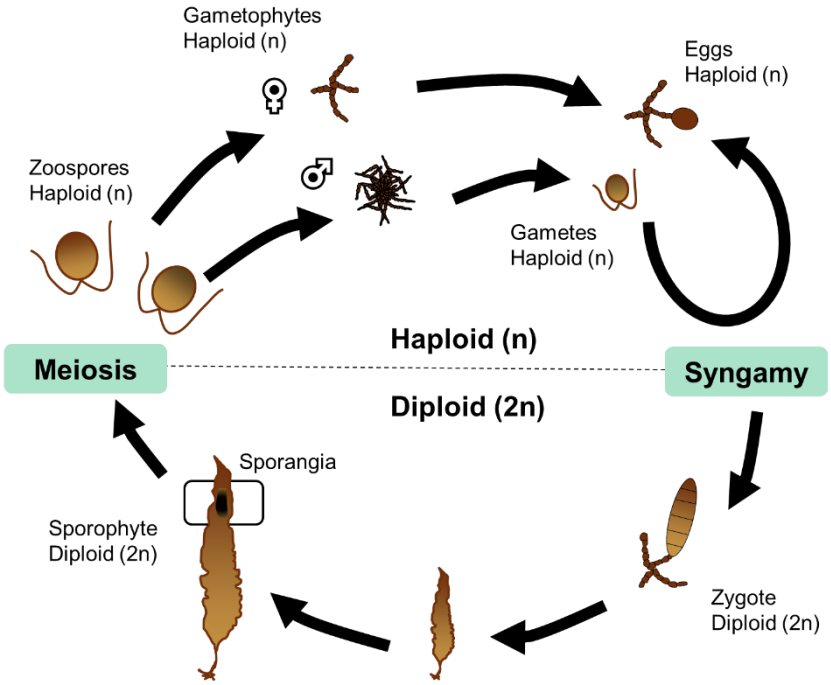


Figure 1. *Saccharina latissima* haplo-diploid life cycle adapted from (Visch et al., 2019).

### 1.1.2. *S. latissima* genetic diversity and phylogeography

In this project, we aimed to pioneer a genome wide association study (GWAS) on *Saccharina* in order to **identify loci** responsible for traits of agronomical interests (such as morphology, biomolecule content, disease resistance…).

Prior to and in parallel to the GENIALG project, a number of studies, all based on microsatellites markers, have unveiled the **population genetics** of *S. latissima* in Europe, at

different geographic scales (Table 1).Two principal sets of microsatellites markers were used in these studies: some developed from expressed sequence tag (EST) are potentially under selection (Guzinski et al., 2016) while the others were developed from genomic DNA (Paulino et al., 2016) can be assumed as neutral. Having such an excellent overview of the distribution and the structuration of *S. latissima* populations across Europe guided our sampling strategy in order to maximise the genetic diversity of the biobank collection.

Table 1. List of studies focusing on *Saccharina latissima* genetic diversity and phylogeography (prior GENIALG and until today).
[1] Same marker(s) than Paulino et *al.* 2016
[2] Same marker(s) than Guzinski et *al.* 2016
[3] Number of wild sporophytes genetically characterised per geographic origin

| **Publication** | **Marker(s)** | **Scale** | **Sites** | **Ind. / site**[3] |
|---|---|---|---|---|
| (Paulino et al., 2016) | Microsatellites (12) | Europe | 3 | 20 |
| (Guzinski et al., 2016) | Microsatellites (32) | Europe | 6 | 16 |
| (Moller Nielsen et al., 2016) | Microsatellites (12)[1] | Denmark | 8 | 23-30 |
| (Luttikhuizen et al., 2018) | Microsatellites (10)<br>Cytochrome c oxidase I | Europe | 8 | 29-33 |
| (Mooney et al., 2018) | Microsatellites (7) | Ireland<br>United Kingdom | 14 | 27-31 |
| (Neiva et al., 2018) | Microsatellites (12)[1]<br>Cytochrome c oxidase I | Europe | 23 | 7-30 |
| (Breton et al., 2018) | Microsatellites (12)[1] | Maine (USA) | 5 | 30-40 |
| (Evankow et al., 2019) | Microsatellites (32)[2] | Norway | 8 | 9-22 |

Overall, *S. latissima* populations show contrasting levels of genetic diversity within-population genetic depending on the set of marker used (EST-derived compared to genomic library derived microsatellites) but no clear pattern of correlation with the latitude could be observed (Guzinski et al., 2016).

Between-populations, *S. latissima* shows a substantial genetic differentiation across Europe that is not simply explained by increasing geographic distances but also by local currents, habitat discontinuity and probably historical demographic events (Moller Nielsen et al., 2016). Connectivity between sites is limited to about 100 km (Guzinski et al., 2016; Moller Nielsen et al., 2016; Neiva et al., 2018) fitting the values published for most kelp species in the review published by (Durrant et al., 2014). Consequently, local adaptation to different environmental conditions (temperature, light, salinity…) is expected to occurr along the range distribution of this species (Guzinski et al., 2016; Moller Nielsen et al., 2016).

From these scientific publications, we chose to compare populations that are separated by more than 100 km and characterized by different environmental conditions of light, temperature and salinity, such as those encountered along their geographic distribution.

Previous GWAS on plants or animals have showed that the sample size to consider could vary between a couple of hundreds to thousand of individuals (Korte and Farlow, 2013; Xiao et al., 2017) depending on multiples factors such as the type of markers used, the size of the genome, the genetic diversity of the species, the ploidy level etc. (Brachi et al., 2011; Korte and Farlow, 2013).

The most significant scientific studies concerning the identification and varietal improvement of kelp species in aquaculture are those concerning *Saccharina japonica* (Table 2), species which represented in 2017, 35% of the algae aquaculture world production and market (FAO, 2018). Those studies, all based on the quantitative trait locus (QTL) identification on two parental sporophytes crossing (also called mapping population or bi-parental population) were able to identify several loci responsible for essential traits in aquaculture such as frond length and frond width.
Base on those two types of studies (i.e. GWAS on plants or animals and QTL on *S.japonica*), the sample size of *S.latissima* for a GWAS analysis should be at least of a couple of hundreds of individuals.

Table 2. Quantitative trait locus (QTL) studies on *Saccharina japonica* mapping population.

| **Genetic marker(s)** | **Phenotype(s)** | **Ind.** | **References** |
|---|---|---|---|
| amplified fragment length polymorphism (AFLP)<br>simple sequence repeat (SSR) | frond length<br>frond width | 92 | (Liu et al., 2010) |
| sequence-characterized amplified region (SCAR) | frond length | 92 | (Liu et al., 2011) |
| amplified fragment length polymorphism (AFLP)<br>sequence-related amplified polymorphisms (SRAPs)<br>simple sequence repeat (SSR) | frond length<br>frond width<br>raw weight<br>frond fascia width<br>frond thickness<br>base shape | 102 | (Zhang et al., 2015) |
| Specific-locus amplified fragment sequencing (SLAFseq) | frond length<br>frond width | 178 | (Wang et al., 2018) |

To summarize, based on the conclusions from these scientific publications, we chose to focus:

1) on the largest geographic distribution of *S. latissima* across Europe,
2) with populations distant of more than 100 km with different environmental conditions,
3) and between a couple of hundreds to a thousand of individuals in total.

## 1.2. *S. latissima* sampling campaign (lead by CNRS and SAMS)

Wild *Saccharina latissima* sporophytes were sampled from populations across Europe (including from the same populations intended to be deployed at some seaweed farms). A unified sampling protocol was developed jointly between CNRS and SAMS (Figure 2), with the aim of harvesting the biological material for WP2 as well as for WP6 - disease monitoring (Task 6.2). When possible, 35 fertile individuals per population were **collected** and phenotyped using photographs and morphometric measurements. Spores released by the fertile part of the sporophyte were used to isolate gametophytes (both in bulk and clonally) and vegetative tissue was kept for further genetic characterisation.

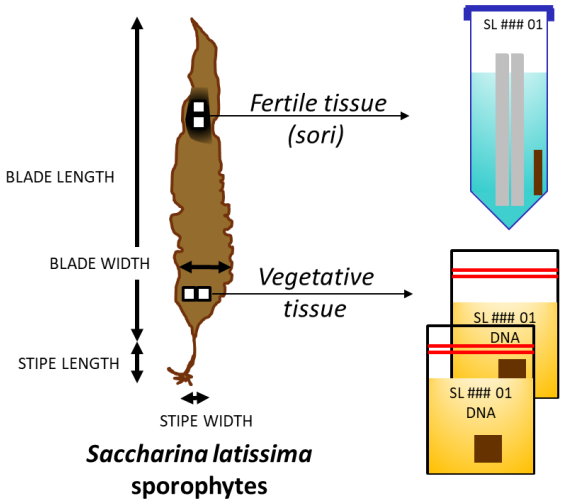


Figure 2. Simplistic schema of a fertile *Saccharina latissima* sporophyte F0 and of the sampling and phenotyping procedure.

A total of **24 populations** were sampled, during either or both **2017-2018** and **2018-2019** seasons i.e. around **800 sporophytes** harvested (Figure 3). The sampling was carried out by GENIALG partners (SAMS, SBR, NUIG, CIIMAR, SINTEF). In addition, we are grateful for the in-kind contribution of Wouter VISCH (University of Gothenburg - Tjärnö) and Inka BARTSCH (Alfred Wegener Institute Helmholtz Centre - Bremerhaven), who arranged access to populations of Sweden and Germany, respectively.

For each sampling event of *S. latissima*, the national regulations pertaining to the **Nagoya Protocol** were followed. When necessary, a prior informed consent (PIC) and/or a mutually agreed terms (MAT) have been initiated by SAMS and shared with the GENIALG collaborator involved, the project leader and the project officer.

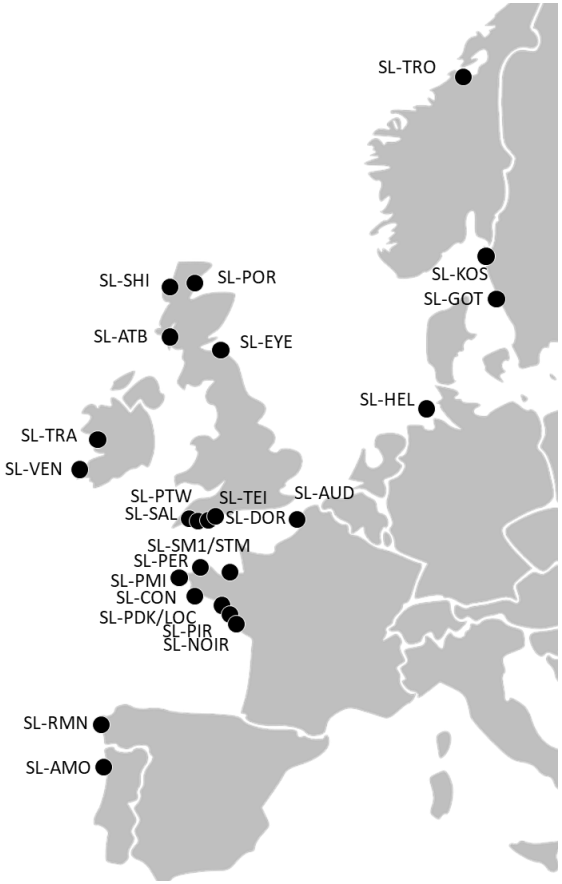


| Sampling year | | Population origine | Pop code | Partners All Nb. Sp F0 sampled | SBR Nb. Sp F0 genotype (microsat) | SBR Nb. Sp F0 phenotype | SBR Nb. Sp F1 genotype (microsat) | SBR Nb. Sp F1 phenotype | SBR Nb. Sp F1 genotype (RADseq) | SAMS/CCAP Nb. Ga Isolation |
|---|---|---|---|---|---|---|---|---|---|---|
| 2017-2018 | FR | Locmariaquer | SL-PDK/LOC | 30 | 30 | 30 | 24 | 24 | 24 | 20 |
| 2017-2018 | FR | Perharidy | SL-PER | 30 | 30 | 30 | 31 | 31 | 31 | 23 |
| 2017-2018 | FR | Saint-Malo | SL-SM1/STM | 19 | 19 | 19 | 15 | 15 | 15 | 19 |
| 2017-2018 | FR | Parc Marin d'Iroise (Lanildut) | SL-PMI | 32 | | 32 | 27 | 27 | 27 | 21 |
| 2017-2018 | FR | Concarneau | SL-CON/PDC | 35 | 35 | 35 | 6 | 6 | 6 | |
| 2017-2018 | NO | Trondheim | SL-TRO | 35 | 35 | 35 | 40 | 40 | 40 | 24 |
| 2017-2018 | UK | Altantic Bridge, Oban | SL-ATB | 35 | 35 | 35 | 13 | 16 | 13 | 24 |
| 2017-2018 | IE | Ventry bay | SL-VEN | 34 | 26 | 34 | 33 | 33 | 33 | 21 |
| 2017-2018 | PT | Amorosa (Porto) | SL-AMO | 30 | 23 | 30 | 29 | 29 | 29 | 23 |
| 2017-2018 | SE | Strömstad | SL-KOS | 35 | 35 | 35 | 41 | 41 | 41 | 24 |
| 2018-2019 | FR | Locmariaquer | SL-PDK/LOC | 9 | 9 | | 18 | 18 | 9 | |
| 2018-2019 | FR | Perharidy | SL-PER | 38 | 20 | 38 | 44 | 44 | 29 | |
| 2018-2019 | FR | Saint-Malo | SL-STM | 35 | | | | | | |
| 2018-2019 | FR | Piriac sur Mer, Loire Atlantique | SL-PIR | 30 | 20 | 30 | 44 | 44 | 24 | 17 |
| 2018-2019 | FR | Noirmoutier, Vendée | SL-NOIR | 30 | 20 | n.d. | 46 | 46 | 15 | 13 |
| 2018-2019 | FR | Audresselles | SL-AUD | 30 | 20 | 30 | 48 | 48 | 26 | 20 |
| 2018-2019 | FR | Concarneau | SL-CON/PDC | 35 | | | | | | 4 |
| 2018-2019 | UK | Sheildaig | SL-SHI | 30 | 28 | 30 | 35 | 35 | 21 | 24 |
| 2018-2019 | UK | Portmahomack | SL-POR | 30 | 28 | 30 | 30 | 30 | 17 | 24 |
| 2018-2019 | UK | Eyemouth | SL-EYE | 30 | 28 | 30 | 36 | 36 | 21 | 24 |
| 2018-2019 | UK | Salcombe | SL-SAL | 10 | | | | | | 6 |
| 2018-2019 | UK | Dorset | SL-DOR | 18 | | | | | | 16 |
| 2018-2019 | UK | Plymouth | SL-PTW | 10 | 10 | | 21 | 21 | 8 | 10 |
| 2018-2019 | UK | Teignouth | SL-TEI | 10 | | | | | | 5 |
| 2018-2019 | IE | Galway | SL-TRA | 30 | 24 | | 16 | 16 | 10 | 17 |
| 2018-2019 | SP | Ria de Muros e Noia | SL-RMN/ESP | 25 | 24 | | 49 | 49 | 24 | 21 |
| 2018-2019 | SE | Göteborg | SL-GOT | 38 | 28 | 38 | 35 | 35 | 19 | 23 |
| 2018-2019 | DE | Helgoland | SL-HEL | 44 | 39 | 44 | 15 | 15 | 10 | |

Figure 3. List of the *Saccharina latissima* populations sampled in 2017/2018 and 2018/2019.
Including the number of individual of the parental generation sampled, genotyped (microsatellite markers) and phenotyped [**Nb. Sp F0**], of the first filial generation genotyped (microsatellite an RADseq markers) and phenotyped [**Nb. Sp F1**], and of the gametophytes isolated which will be available in SAMS Culture Collection (CCAP) [**Nb. Ga**].

## 1.3. Genome wide association studies (GWAS) on *S. latissima* sporophytes (by CNRS)

One key objective of GENIALG is to apply modern breeding approaches to the two target cultivated seaweed species in order to improve aquaculture yields, product quality and losses due to abiotic and biotic factors. The genome-wide association study approach aims to exploit natural genetic diversity to identify alleles associated with traits of interest for aquaculture. Contrarily to older breeding methods, this approach allows to capture a larger portion of species-wide variation and to identify markers significantly associated with a phenotype that should be much closer to the causal variant than is the case in a bi-parental population. The strain collection and biobanking described in this deliverable represents a crucial first step towards the implementation of the GWAS approach.

### 1.3.1. Experimental set up aiming to obtain the F1 sporophytes from F0 sporophytes.

The experimental protocol developed for the *S. latissima* GWAS experiment on sporophytes was composed of four main stages: i) collection of sporophytes from parental strains from a broad range of European populations [SP F0], ii) self-fertilization (selfing) of gametophytes collected from each parental individual [GA], iii) growth of sporophytes derived from selfing procedure under standardized conditions [SP F1] and finally iv) phenotyping of growth traits (Figure 4).

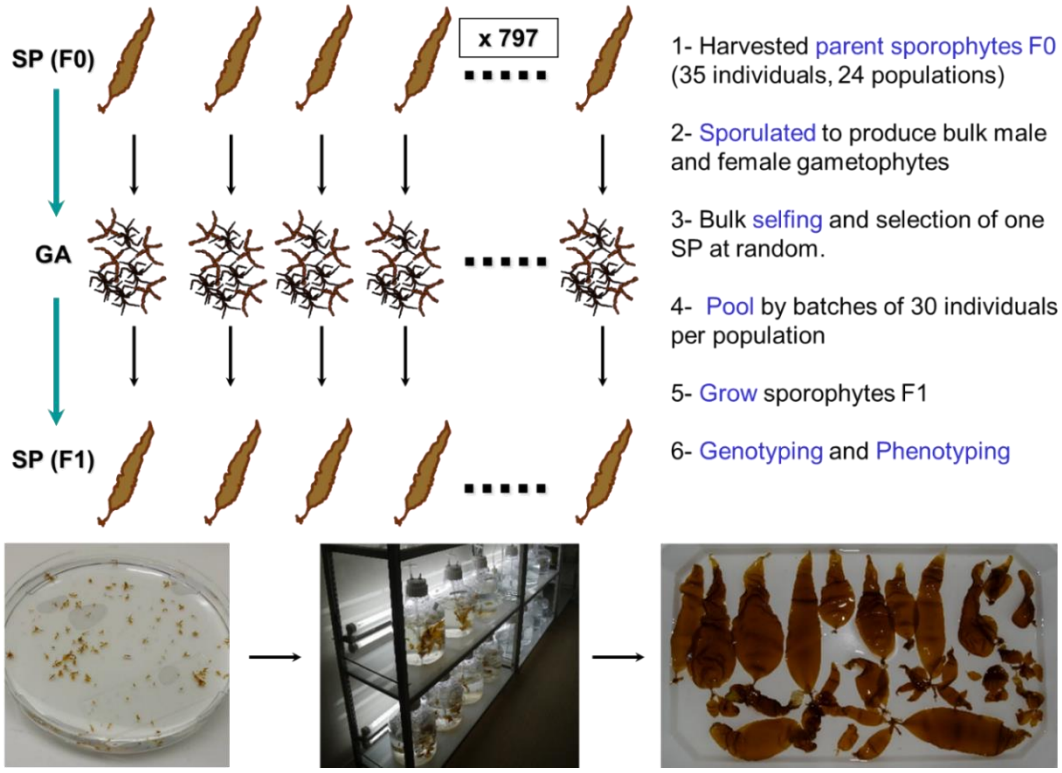


Figure 4. GWAS experimental design on *S. latissima* sporophytes.

The maintenance of standard and equal environmental conditions is essential during the culturing of F1 sporophytes. A set of standardised procedures were applied to minimise any bias associated with unequal conditions of growth among the different F1 strains. All the F1 sporophytes in this experiment were maintained for 30 days in culture with the same volume of seawater (10 L flasks), the same amounts of nutrients, light intensity and light exposure. In addition, two sporophytes per strain (up to max 10 strains per flask) were admixed in the same flask and cultured under the same conditions (Figure 4).

### 1.3.2. Phenotyping the F1 sporophytes

The phenotypic description of *Saccharina latissima* was extrapolated from five main measures (Figure 2) that are directly linked with the natural morphology of this kelp species:

i) Stipe length (measured between the end of the holdfast and the basis of the meristem)
ii) Total length (sum of stipe and blade lengths)
iii) Blade length (measured from the meristem to the end of the blade in the most linear way)
iv) Blade width (measured at the largest section of the kelp blade)
v) Blade surface

At the time of collection, F1 individuals (i.e. first filial generation) were placed on an overhead projector with a neutral background, sufficiently spaced from each other to limit any potential overlap. A scale bar was placed near each set of sporophytes before taking a high-quality photograph. The length and surface associated with the five mentioned phenotypes were obtained by the software ImageJ2 (Rueden et al., 2017). The same scale bar was used as a reference to compare measurements of individuals from different photographs.

### 1.3.3. Genotyping the F0 and F1 sporophytes with microsatellite makers.

**Objectives:** The genotype data obtained were utilised for two main purposes:
1) The characterisation of the different populations of *S. latissima* collected, in order to understand the effect of population stratification and the boundaries among the different sampled wild populations.
2) An assignment test of parental/offspring *S. latissima* after the breeding protocol used for the GWAS experiment (see detail here below).

Within the GENIALG WP2 Task 1.2 microsatellite markers were applied in order to characterize the genetic diversity of the collected *S. latissima* strains. This approach required the genotyping of both parental (F0) ($N_{FO}$ = 724) and offspring (F1) ($N_{F1}$ = 696) individuals with a panel of 28 microsatellite markers. This task was performed at the facilities of the SBR (CNRS).
The GWAS experiment is based on the identification of genomic features linked to phenotypic variations in a model. Hence, genotyping of thousands of genome-wide SNPs markers allows

phenotypic variation (e.g. growth traits) to be related to specific markers located nearby QTL regions of the *S. latissima* genome that might functionally explain the observed variation. It is therefore crucial to understand the role of population stratification in the set of strains utilised in order to correct the GWAS and deal with bias due to the life histories of the sampled individuals. The whole set of parental strains, obtained from 24 different locations, was examined with microsatellite markers (SSRs) and the genotypes obtained for 28 SSRs specifically designed from the *S. latissima* genome. These data were utilised to perform analysis of population structure.
The information concerning the population structure derived from the SSRs analysis for the F0 individuals and the methodology set for the assignment test between F0/F1 will be also applied to the GENIALG Task 6.4 (gene flow between wild and farmed *S. latissima*) to determine the proportion of genetic diversity in farmed *Saccharina latissima* retained from local wild (F0) populations and the occurrence of detection of “migrants” originated from non-proximal wild populations to the farmed ones.

### 1.3.4. Genotyping the F0 and F1 sporophytes with ddRAD-seq markers.

After phenotyping, each F1 individual was genetically characterized with a panel of 28 microsatellite markers. An assignment test allowed the multilocus genotypes of the parental strains to be compared with the generated F1 strains and hence identify the population of origin of each F1 individual. This information allowed the selection of the F1 individuals for the preparation of two double-digest restriction-site associated DNA sequencing (ddRAD-seq) genomic libraries (one represented by 233 individuals and the other represented by 261 individuals) currently ready to be submitted to an external genomic service for sequencing.

## 1.4. Genome wide association studies (GWAS) on *S. latissima* gametophytes (by SAMS)

To our knowledge, only one single recent paper (Khan et al., 2018) has been published on the topic of breeding, disease resistance and algae (https://www.ncbi.nlm.nih.gov/pubmed/). In comparison, more than 1 700 and 3 700 scientific studies have been published since 1990 on animals and plants, respectively (Figure 5).

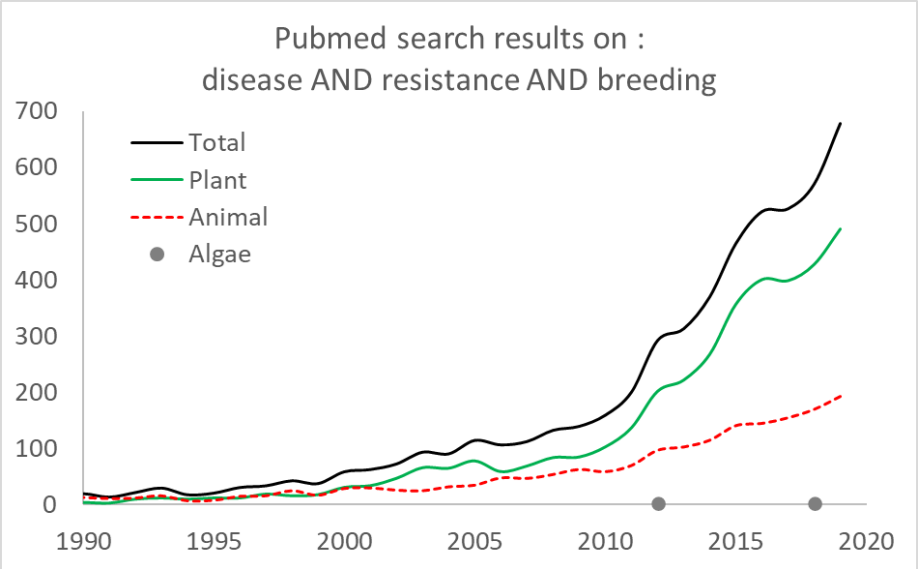


Figure 5. Results by year of NCBI/PubMed publications with the search term "disease AND resistance AND breeding" either with Plant, Animal, Algae or in Total.

However, in aquaculture (and as well as for any industry) pathogens are responsible for major economic loss. As an example, three main diseases (Oomycetes and virus) are impacting the *Pyropia* (Rhodophyta) aquaculture with an economic annual loss of more than US $10 million just in Korea (Kim et al., 2014) between the loss of the production, the algae price drop and the disease control cost (up to 62% of a sea farm running cost). We chose to focus on Oomycetes, one of the most devastating pests in aquaculture and agriculture (Badis et al., 2019; Derevnina et al., 2016; Kamoun et al., 2015).

Our goal is to start to fill this knowledge gap and to identify, in genomes of algae, loci responsible for resistance to disease such as oomycetes or endophytes. As a starting point, previous studies have shown, on the brown algae model *Ectocarpus* that different individuals show different degree of resistance against such pathogen (Gachon et al., 2009). Preliminary data obtained prior to GENIALG suggested that disease resistance is a quantitative trait transmissible from parent to offspring i.e. genetically inheritable (Martina Strittmatter, personal communication).

For this, the level of resistance against a pathogen must be quantified for each *Saccharina latissima* individual and correlated with its own genetic diversity. To identify loci involved in *S. latissima* disease resistance, clonal gametophyte have been isolated from the 700 wild

sporophytes thus allowing to quantify the level of resistance in controlled conditions and a miniaturised, parallelisable laboratory assay.

### 1.4.1. Experimental set up

For each collected fertile *S. latissima* sporophyte (F0), zoospore release was induced at SAMS or at CNRS and bulked gametophytes later shared between the two GENIALG partners. Individual young male and female gametophytes were isolated manually (starting from 6 of each per sporophyte) at SAMS and grown up in culture to obtain enough biomass (few months up to more than a year) for the phenotyping, genotyping and biobanking (cryopreservation).

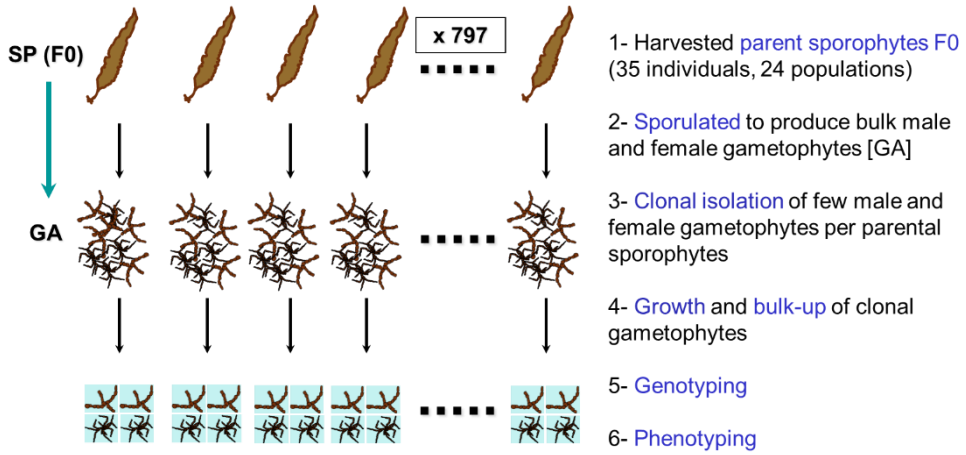


Figure 6. GWAS experimental design on *S. latissima* gametophytes.

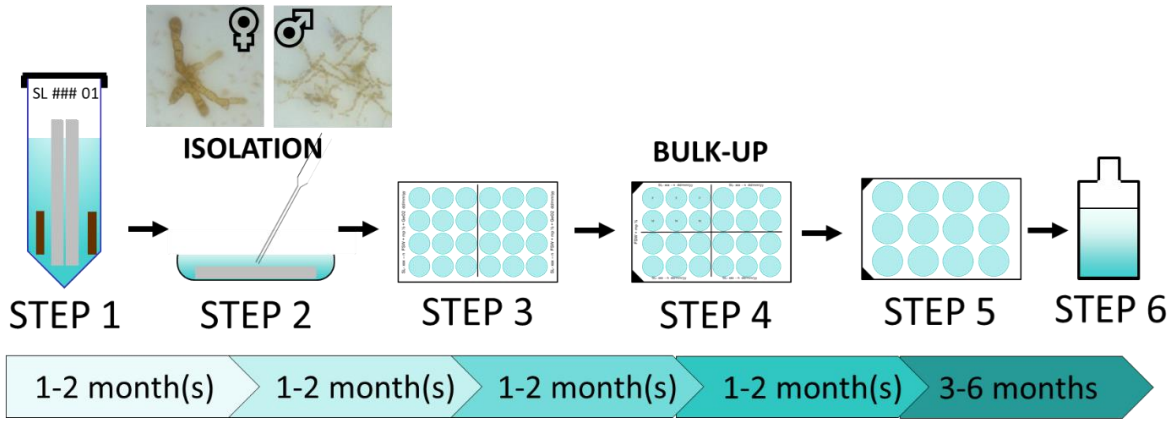


Figure 7. Isolation and bulk-up procedure for *Saccharina latissima* gametophytes.
From fertile sporophytes until obtaining clonal gametophyte cultures with enough biomass for the phenotyping, genotyping and biobanking (cryopreservation).

### 1.4.2. Development of a phenotyping assay to quantify the resistance against Oomycete pathogens.

Due to the extremely slow growth rate of *S. latissima* gametophytes, a quantitative and parallelisable assay for disease resistance against the oomycete pathogen *Anisolpidium ectocarpii* was first developed using the fast growing, filamentous model brown alga *Ectocarpus.* Indeed, diseases phenotyping methodologies in filamentous brown algae (Calmes et al., 2020) and a genetic map of *Ectocarpus* segregating population (Avia et al., 2017) are available, which facilitated a starting point to develop high throughput phenotyping for disease resistance in this algae model.

We combined different approaches based on host's PAM fluorometry and chlorophyll autofluorescence, coupled with pathogen's chitin fluorescence (WGA-FITC) and relative DNA quantification (qPCR) linked with the WP6 (disease monitoring) in order to monitor detectable changes during the course of the infection. We initially tested two strains, Ec568f and Ec32m, which display contrasting resistance to *A. ectocarpii* AnQU 67-5 strain (Murua, in prep).

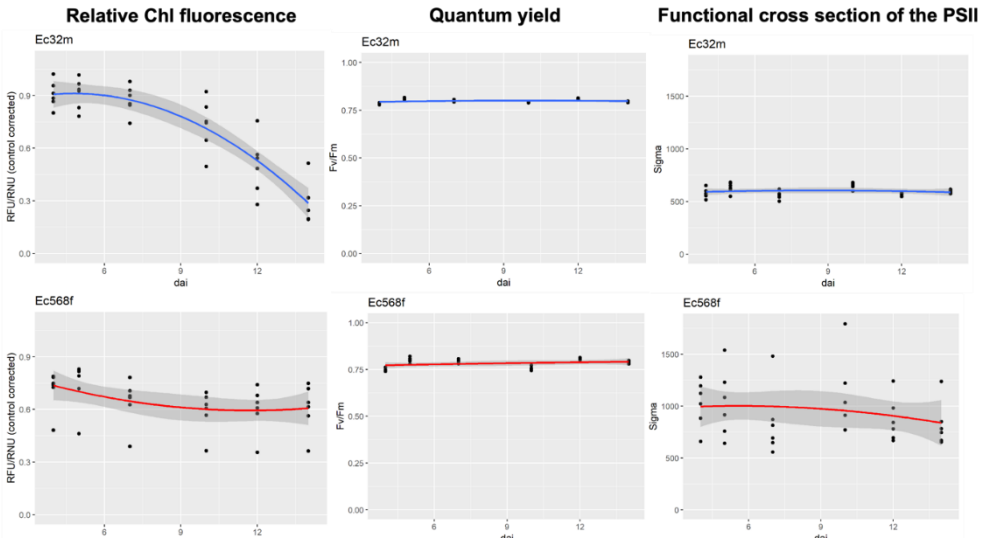


Figure 8. Time point measurements of *Ectocarpus* Ec32m (susceptible, in blue) and Ec568f (resistant, in red) strains, after a challenge by the oomycete *Anisolpidium ectocarpii.*
Whereas some proxies showed some marked temporal tendencies and differences between both parental strains (e.g. ratio between relative fluorometric units RFU and relative nephelometric unit RNU), some others were constant (quantum yield) and/or oddly variable overtime (functional cross section of the PSII).

**Non-invasive, continuous monitoring of disease progress.**
As show in the Figure 8, results show that chlorophyll is an excellent to track infection if corrections for biomass (i.e. nephelometry) is performed. Furthermore, Fo and Fm values (fluorescence of photosystem II) are promising because of their strong variation in *Anisolpidium* challenged *Ectocarpus*. On the other hand, PAM fluorometry proxies normally used in physiology (e.g. quantum yield) do not capture subtle differences during infection.

**Destructive, end-point measurement of the pathogen colonisation.**
At the end of the infection time-course, stained chitin fluorescence is excellent to quantify the degree of infection (corrected with the biomass). On the same samples of *Ectocarpus* challenged by *Anisolpidium*, it is also possible to quantify by qPCR both pathogen and host DNA to obtain a relative abundance of the pathogen (Figure 9).

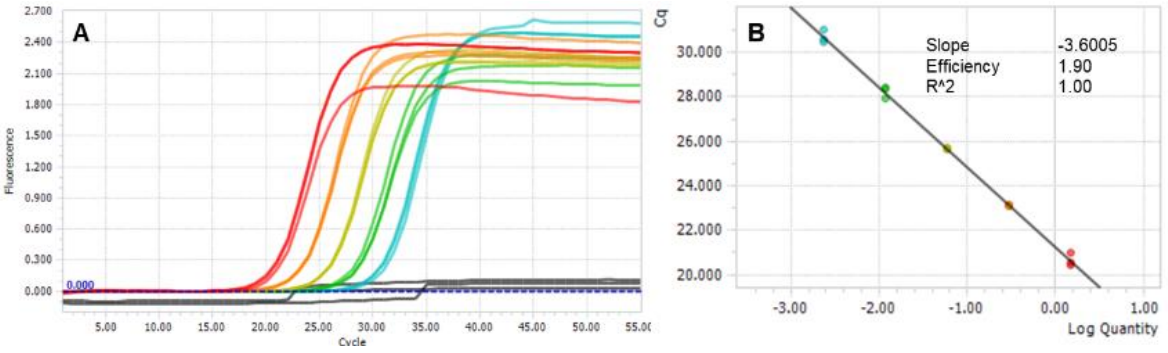


Figure 9. Molecular quantification test of the brown algae pathogen *Anisolpidium ectocarpii*. The DNA amplification curves of *A. ectocarpii* DNA gradient show a linear correlation between the logarithm of the DNA quantity and the cycle quantification value (Cq).

In total, four of the tested proxies are applicable to the same experimental set up at different time points: two during the time course on the infection (relative chlorophyll florescence and fluorescence of photosystem II) and two at the end of the disease progress (chitin fluorescence and relative DNA quantification).

**Proof of concept – detection of QTLs associated to disease resistance in *Ectocarpus*.**
To evaluate and validate the usefulness of the proxies developed above, we took advantage of the unexpected fact that our two *Ectocarpus* strains with different degrees of resistance to *A. ectocarpii* have been crossed to generate a progeny of ca. 90 individuals and build *Ectocarpus* genetic map (Heesch et al., 2010).

So far, each of these ca. 90 strains has been phenotyped with at least six replicates. We are currently developing an R-coded script able to i) transform and read the output files coming from the different equipment used for this phenotyping, ii) extract the key information and correct/normalise data needed to develop accurate infection proxies and iii) detect potential outliers. In the end, we aim to create a final matrix with all the relevant proxies to later link them with the available genetic map in order to find and characterize QTLs related with disease resistance.

This phenotyping assay will further be applied on a few hundreds of clonal *Saccharina latissima* gametophytes after the Covid-19 lockdown. Those data, combined to the genetic diversity information, should allow us to identify loci involved in biotic stress resistance in wild populations.

### 1.4.3. Genotyping *S. latissima* gametophytes.

As previously mentioned, 423 clonal gametophytes of *S. latissima* are maintained, sub-cultured and scaled-up on a regular basis. They will be genotyped using the same ddRAD-seq protocol as established for the sporophytes (by CNRS), after the Covid-19 lockdown.

### 1.4.4. Biobanking and cryopreservation of *S. latissima* gametophytes

Whenever possible, 12 clonal gametophytes males and 12 females were bulked-up in culture for each *S. latissima* population sampled. Each gametophyte was from a different wild sporophyte (SP F0). In total, a collection of 423 clonal gametophytes are currently maintained at SAMS (Figure 3) and will be deposited in CCAP using the cryopreservation protocol developed by (Visch et al., 2019) (Figure 10).

Briefly, *S. latissima* male and female clonal gametophytes were successfully cryopreserved using DMSO (5%) as a cryoprotectant and a two-step cryopreservation protocol. The controlled-rate cooling methods generated higher viability than the low-tech passive cooling methods, but both methods resulted in viable gametophytic cells with the ability to successfully complete its life cycle.

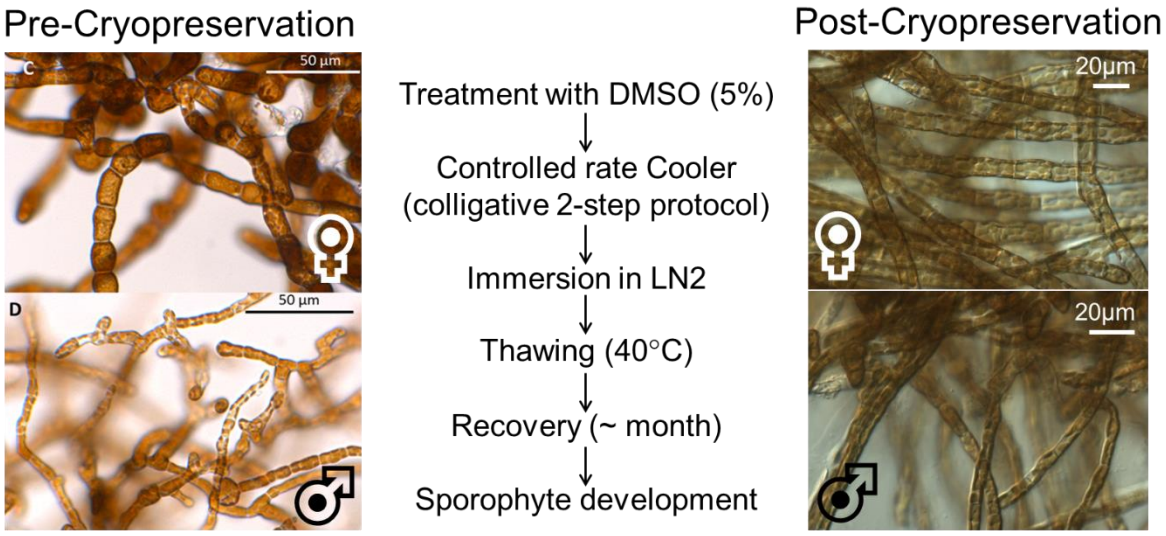


Figure 10. Cryopreservation protocol to preserve *Saccharina latissima* gametophytes

A new cryotank (Taylor-Wharton LS6000, Wolf Labs) was acquired to keep the *S. latissima* cryopreserved biobank and it is now stored in CCAP cryo store facility. The cryotank has now been added to CCAP internal cryo database, which registers all the information regarding the cryopreservation protocol for each strain. Everything is now in place to initiate the cryopreservation of the clonal gametophytes after the Covid-19 lockdown.

# 2. *Ulva* spp.

## 2.1. Introduction

### 2.1.1. *Ulva* spp. life cycle

Like *Saccharina latissima*, *Ulva* spp. has a digenetic haplo-diploid life cycle. The diploid sporophyte produces meiotic sporangia in the oldest part of the thallus (i.e. the most external part) and release haploid tetraflagellate zoospores (Figure 11). These spores will develop into haploid either male or female gametophytes, which are morphologically similar to the diploid sporophyte. Fertile female and male *Ulva* gametophytes release biflagellate gametes which fuse to form a quadriflagellate zygote which then germinates into a diploid sporophyte. Unlike *S. latissima,* sporophytes and gametophytes are isomorph stages i.e. they are morphologically identical.

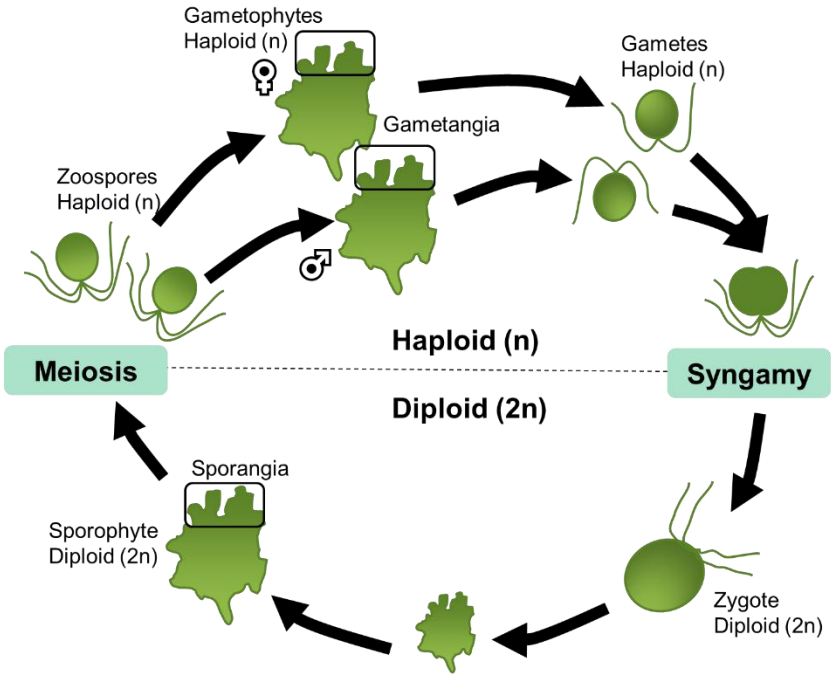


Figure 11. *Ulva* spp. haplo-diploid life cycle adapted from (Wichard, 2015).

### 2.1.2. *Ulva* spp. genetic diversity and phylogeography

*Ulva* spp. represent a diverse group of green macroalgae species, containing some 131 laminar and tubular species currently accepted taxonomically. *Ulva* is present throughout the world's seas and oceans, with several species commonly found within the same areas (Fort et al., 2020). Despite the large number of species described in the literature, often only subtle morphological differences allow to distinguish species (Lee et al., 2019), with some of those "morphological markers" showing degrees of plasticity due to the environment (Loughnane et al., 2008). Furthermore, *Ulva* classification is constantly evolving as new studies shed light to

the genetic diversity of *Ulva* species (Hayden et al., 2003; Steinhagen et al., 2019). Only DNA-based identification can conclusively distinguish *Ulva* species, assuming that the sequencing information of public repositories is accurate, which is not the case for *Ulva* (Hughey et al., 2019). Hence, the precise phylogeographic distribution of *Ulva* species remains to be thoroughly investigated, and new assays to quickly, cheaply and accurately determine *Ulva* species would be beneficial (Loughnane et al., 2008).

## 2.2. *Ulva* spp. sampling campaign (lead by NUIG)

The sampling campaign focused on laminar *Ulva* spp., which are the most relevant group of species for aquaculture (Bolton et al., 2009; Lopes et al., 2019; Shpigel et al., 2017). Our sampling strategy was intentionally blind to species identity. This blind approach allowed i) comparisons of the growth potential of the different laminar *Ulva* species and ii) characterisation of the population genetics of laminar *Ulva* of the North East Atlantic coast. Sampling was performed by some of the GENIALG partners: NUIG, SAMS, SBR, WUR, CIIMAR and ALGAplus. In total 543 strains were sent to NUIG, of which 220 have been phenotyped and genotyped (whole genome sequencing and/or barcoding). The geographical location and originating contributor are shown in Figure 12. For *Ulva* strain selection and the genome wide association study (cf. section 2.5), all strains were maintained in NUIG as per (Fort et al., 2019).

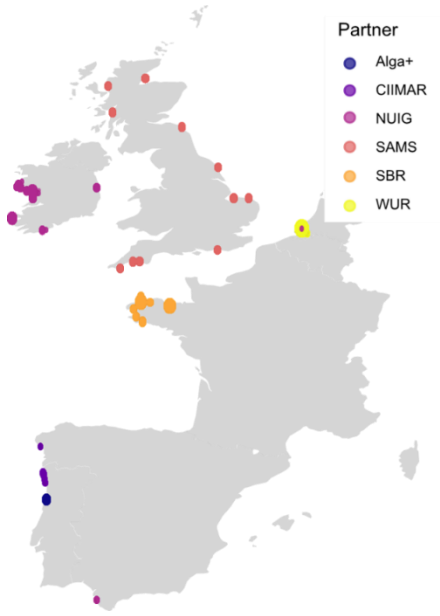


Figure 12. *Ulva* collection sites as part of the Genome Wide Association Study.

For each sampling event of *Ulva* spp., the national regulations pertaining to the **Nagoya Protocol** were followed, and where needed a MTA signed between partners.

As an example, UAVR and ALGAplus collaborated in the preparation of samples of *Ulva* spp.to be sent to GENIALG partners for phenotyping, genotyping, and biobanking. Strains R1 to R17 were collected by ALGAplus, at different points in the production facilities of the company, including strains from natural blooms and strains in cultivation. Strains R18-R26 were collected

by UAVR from wild populations blooming at different locations in the Ria de Aveiro lagoon (Table 3). Figure 13 shows the approximate location of all the samples collected so far in Ria de Aveiro.

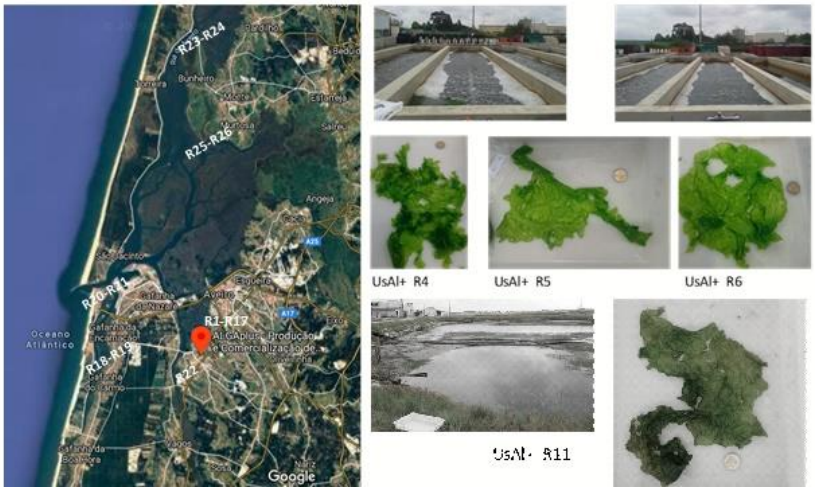


Figure 13. Location and samples example collected of *Ulva* spp. collection sites at ALGAplus and in Ria de Aveiro.

Table 3. Information about the *Ulva* samples collected in 2018-2019 by UAVR and ALGAplus. All strains are kept and maintained in the biobank set at ALGAplus laboratory.

| Replicate | Species | Code | Date |
|---|---|---|---|
| R1 | *Ulva rigida* | UsAL+ | 07/2018 |
| R2 | *Ulva rigida* | UsAL+ | 07/2018 |
| R3 | *Ulva rigida* | UsAL+ | 07/2018 |
| R4 | *Ulva rigida* | UsAL+ | 07/2018 |
| R5 | *Ulva rigida* | UsAL+ | 07/2018 |
| R6 | *Ulva rigida* | UsAL+ | 07/2018 |
| R7 | *Ulva rigida* | UsAL+ | 07/2018 |
| R8 | *Ulva rigida* | UsAL+ | 07/2018 |
| R9 | *Ulva rigida* | UsAL+ | 07/2018 |
| R10 | *Ulva rigida* | UsAL+ | 07/2018 |
| R11 | *Ulva rigida* | UsAL+ | 07/2018 |
| R12 | *Ulva rigida* | UsAL+ | 07/2018 |
| R13 | *Ulva rigida* | UsAL+ | 07/2018 |
| R14 | *Ulva rigida* | UsAL+ | 07/2018 |
| R15 | *Ulva rigida* | UsAL+ | 07/2018 |
| R16 | *Ulva rigida* | UsAL+ | 07/2018 |
| R17 | *Ulva rigida* | UsAL+ | 07/2018 |
| R18 | *Ulva* spp. | 1-Us-CM | 07/2019 |
| R19 | *Ulva* spp. | 2-Us-CM | 07/2019 |
| R20 | *Ulva* spp. | 3-Us-B | 07/2019 |
| R21 | *Ulva* spp. | 4-Us-B | 07/2019 |
| R22 | *Ulva* spp. | 5-Us-CI | 07/2019 |
| R23 | *Ulva* spp. | 6-Us-PV | 07/2019 |
| R24 | *Ulva* spp. | 7-Us-PV | 07/2019 |
| R25 | *Ulva* spp. | 8-Us-CB | 07/2019 |
| R26 | *Ulva* spp. | 9-Us-CB | 07/2019 |

Small blade portions were prepared following the protocol provided by NUIG (Figure 14). Briefly, cultures of *Ulva* were prepared by selecting small blade portions that were stored in seawater in falcon tubes (Figure 14). For **biobanking**, small pieces of blades (50 mm x 50 mm) were prepared and stored in flasks with VSE culture media, under dim light and with no aeration, at 13°C, 8:16 h light:dark period. Samples of most strains have been sent to NUIG for **phenotyping**. All strains collected during 2018 and 2019 by UAVR and ALGAplus are now being maintained the biobank of ALGAplus.

Figure 14. Sample preparation protocol for *Ulva* spp. biobanking and phenotyping provided by NUIG. 1) Sample of *Ulva* spp.; 2-3) Subsample of 100 x 100 mm cut from a sample *Ulva* spp., stored in plastic Falcon tubes with filtered seawater and sent to NUIG partner; 4-5) Subsample of 50 x 50 mm cut from a sample of *Ulva* spp. for biobanking. Sectioned pieces were washed three times with filtered seawater and stored in flasks with autoclaved filtered seawater and VSE culture media. 6-8) Biobanking subsamples stored in flasks, in the SD chamber at 13ºC and 8L:16D photoperiod. ©ALGAplus

Data on frond size, texture, colour, epiphytes and reproductive status was collected from sampled individuals of strains R6; R11 and R13 during visual quality controls, at ALGAplus. All strains presented perforated blades of a small to medium size area (chart sizes 3-4, Table 4) that tear easily (Figure 15). Blades were estimated predominantly as level 7 coloration according to the pantone scale 390U in relation to tissue nitrogen (Figure 16) (Robertson-Andersson et al., 2009). Individuals did not present significant epiphytes apart from occasional diatom light coverage.

Table 4. Visual quality control size chart for *Ulva rigida* according to frond size diameter largest and shortest axis (E1; E2) in cm.

| E1/E2 | <5cm | 6-10cm | 11-20cm | >20cm |
|---|---|---|---|---|
| < 5cm | 1 | 2 | 3 | 4 |
| 6-10cm | 2 | 4 | 6 | 8 |
| 11-20cm | 3 | 6 | 9 | 12 |
| >20cm | 4 | 8 | 12 | 16 |


Figure 15. Visual quality control of three sampled individuals of selected strains of *Ulva rigida*: R6, R11 and R13, respectively. ©ALGAplus

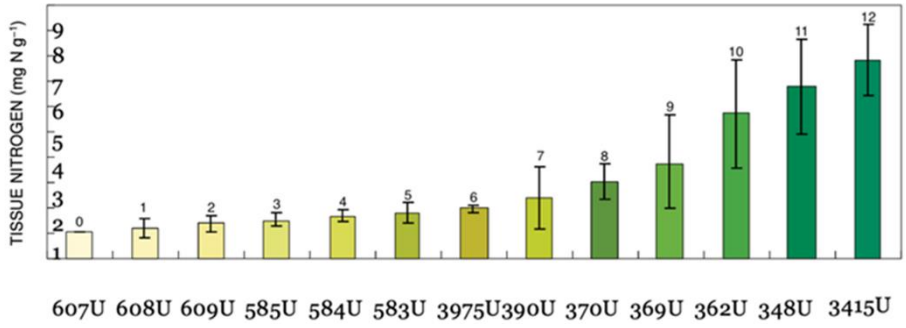


Figure 16. Relationship between tissue nitrogen (mg.g$^{-1}$) and thallus colour for *Ulva lactuca*, shown by Pantone® matt colour labels (n = 600).
Print or online representation of the Pantone® colours in the figure is as precise as technical constraints permit (Robertson-Andersson et al., 2009).

The observation of swarmers was detected once under light microscopy indicating a sporulation event on strain R11. Swarmers were described as tetra-flagellated and oval shaped, forming cluster groups of 6-12+ within each cell compartment, seen in Figure 17. Both vegetative and reproductive cells were observed in the sporulating individual therefore it is likely that other events have been present but undetected. Perforated individuals have been linked to both sporulating and bleaching events with the presence of brown granules within cells, samples currently being investigated by SAMS (link with the WP6 - disease monitoring).

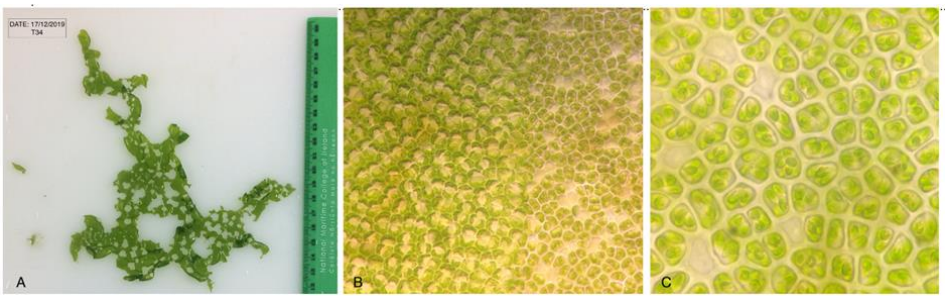


Figure 17. Strain R11 with fertility signs.
(A) macroscopic individual scaled with ruler; and under light microscopy: (B) transition zone between vegetative and reproductive cells 100x; C) clustered swarmers within cell compartments 400x. ©ALGAplus

## 2.3. Performance assessment of *Ulva* strains (by ALGAplus, link with WP3)

Strains have been sent to NUIG for phenotyping and, among these strains, Al+R6, Al+R11 and Al+R13 from ALGAplus exhibited the **best growth performances** based on phenotyping results, information received from NUIG partner. Using vegetative propagation techniques, part of the biomass of the three selected strains plus Al+R12 was transferred from the biobank into actively growing cultures. These were initially grown under a short-day photoperiod and later under long-day conditions to accelerate growth. During this period, inside culture chambers, cultures were sequentially transferred into larger culture units with weekly maintenance protocols, until enough biomass was available to transfer to the experimental outdoor tank system (230L capacity) in August 2019. The cultures in these 230L tanks are still being kept today with healthy biomass, with no need of restocking since Time 0 (Figure 18).

In October 2019, it was possible to set one commercial size tank (20m$^3$) per strain. The three strains were kept until mid-December, with average yields ranging from 0.7-1.1 kg (ww)/m$^2$/week. At this point (April 2020), only strain Al+R11 was able to withstand the conditions of the commercial size operation and is currently being kept in two 20m$^3$ tanks, waiting to be transferred to the new raceways system (WP3). Stocking density and water renewal rates are the same one used for routine production operations at the farm. Monitoring is now done every two weeks and average yield is 1 kg (ww)/m$^2$/week. This is higher than the average yield at ALGAplus currently at 3 kg/m$^2$/month (3 years measurements). Final comparisons and conclusions on growth performance and chemical composition between this optimized selected strain (Al+R11) and commercial strains will be performed (link with the WP3).
Throughout the cultivation trial, quality control measurements were done weekly to observe changes in morphology as well as the presence of pests or epiphytes. A photographic record was kept, and a few samples were sent to SAMS to identification of possible biological contaminants (link with the WP6 Disease monitoring).


Figure 18. Detail of selected *Ulva* strains at different steps of the biomass production process.
A. Beginning of the biomass production process, indoor. B. During the biomass production process, indoor. C. Outdoor cultivation tanks for *Ulva* at ALGAplus.

Phenotyping carried out by UAVR also included detailed analysis of **biochemical** and **lipidomic signatures** of collected strains in different sampling sites. The high-throughput analysis of the entire collection was accomplished by using the Liquid Chromatography-Mass Spectrometry (LC-MS) based-platform at Aveiro.

*Ulva* spp. biomass collected along Portugal and Spain Atlantic coastline was phenotyped to detect variability of their biochemical composition and lipidome. Different species and/or strains of *Ulva* were sampled from nine different geographic locations. *Ulva* spp. was sampled from eight distinct ecosystems along the Atlantic Iberian coast and *Ulva rigida* comes from ALGAplus (Figure 19, Table 5). We also investigated the hypothesis that lipidomic signatures can be used to trace the geographic origin post-harvesting of these valuable green seaweeds. These samples were screened for their moisture, ash, protein, and lipid content that was profiled by LC-MS.

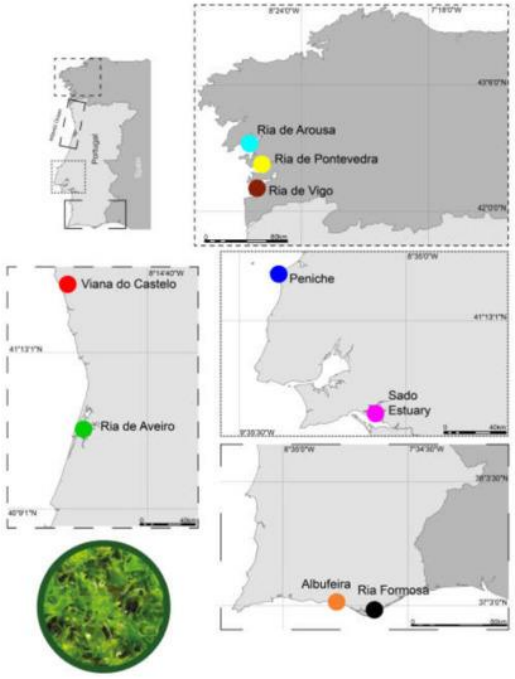


Figure 19. *Ulva* spp. sampling sites along Portugal and Spain Atlantic coastline.

Table 5. *Ulva* spp. sampling sites in different places of the Portuguese coast.

| **Species** | **Code** | **Origin** |
|---|---|---|
| *Ulva* spp. | RAr | Ria Arousa |
| *Ulva* spp. | RPo | Ria de Pontevedra |
| *Ulva* spp. | RV | Ria de Vigo |
| *Ulva* spp. | VC | Viana do Castelo |
| *Ulva* spp. | RAv | Ria de Aveiro-ALGAplus |
| *Ulva* spp. | Pe | Peniche |
| *Ulva* spp. | SE | Sado Estuary |
| *Ulva* spp. | Al | Albufeira |
| *Ulva* spp. | RF | Ria Formosa |

Biochemical composition expressed as **total lipids, protein, minerals (as ash), carbohydrate** and **other compounds** varied extensively between *Ulva* spp. from different geographical origins (da Costa et al., 2020) (Table 6). Total lipids content (%DW) ranged from 0.34 ± 0.06% DW (in RF) to 1.77 ± 0.07% DW (in RP) (a 5.2-fold variation in lipid content). No significant differences were found between total lipid content from RF, RV, SE, and RAv specimens, which displayed the lowest lipid content; lipid content in *Ulva* spp. collected in Pe

and RP displayed the highest lipid yields (>1% DW) and did not differ significantly between these two locations. There were also differences in protein and ash contents displayed by *Ulva* spp. originating from different locations. Protein content ranged from 4.70 ± 0.31% DW (in RV) up to 18.13 ± 1.26% DW (in Pe), while ash ranged between 13.48 ± 0.80 %DW (in SE) up to 27.79 ± 2.51% DW (in RAv). Total carbohydrate and other constituents also displayed significant differences across different locations and ranged from 53.36 ± 1.30 % DW (in Pe) up to 78.67 ± 0.31% DW (in RF) (Table 6). Differences observed in the biochemical composition with origin encouraged the in depth-study of lipid profiles, at a molecular level, to better understand adaptive lipid profiling and biomarkers discovery of *Ulva* spp. between different geographic origins.

Table 6. Biochemical composition of *Ulva* spp. specimens.
Labels of the sites are according to the notation: Albufeira (Al), Peniche (Pe), Ria Arousa (RAr), Ria de Aveiro (RAv), Ria Formosa (RF), Ria de Pontevedra (RP), Ria de Vigo (RV), Sado Estuary (SE), and Viana do Castelo (VC), mean ± s.d. % (n=5)

| | **Lipid content** | | **Protein** | | **Carbohydrates and others** | | **Minerals (as ash)** | |
|---|---|---|---|---|---|---|---|---|
| **Code** | **Mean %** | ± s.d. % | **Mean %** | ± s.d. % | **Mean %** | ± s.d. % | **Mean %** | ± s.d. % |
| Al | **0.51** | 0.06 | **9.08** | 0.41 | **71.93** | 1.62 | **18.48** | 1.92 |
| Pe | **1.20** | 0.28 | **18.13** | 1.26 | **53.36** | 1.30 | **27.31** | 0.82 |
| RAr | **0.50** | 0.12 | **6.59** | 0.34 | **67.49** | 1.59 | **25.42** | 1.57 |
| RAv | **0.40** | 0.07 | **8.55** | 0.29 | **63.26** | 2.40 | **27.79** | 2.51 |
| RF | **0.34** | 0.06 | **6.23** | 0.27 | **78.67** | 0.31 | **14.77** | 0.09 |
| RP | **1.77** | 0.07 | **9.90** | 0.84 | **66.16** | 3.95 | **22.17** | 3.91 |
| RV | **0.47** | 0.08 | **4.70** | 0.31 | **69.20** | 1.41 | **25.63** | 1.26 |
| SE | **0.39** | 0.13 | **12.57** | 0.48 | **73.56** | 1.15 | **13.48** | 0.80 |
| VC | **0.64** | 0.05 | **8.60** | 0.18 | **70.57** | 0.53 | **20.19** | 0.41 |

Regarding the lipid profiling obtained by LC-MS, 201 molecular species were identified and semi-quantified, distributed between the glycolipids classes (monogalactosyl diacylglyceride, MGDG; digalactosyl diacylglyceride, DGDG; sulfoquinovosyl monoacylglyceride, SQMG; sulfoquinovosyl diacylglyceride, SQDG), phospholipids (phosphatidylcholine, PC; lyso-PC, LPC; phosphatidylglycerol (PG), lyso-PG (LPG), phosphatidylinositol (PI), phosphatidylethanolamine (PE), lyso-PE (LPE), and betaine lipids (monoacylglyceryl and diacylglyceryl-N,N,N-trimethyl homoserine, MGTS and DGTS). The natural variation in the lipidome of *Ulva* from different geographic places, from pooled samples collected in July 2018, was addressed by multivariate exploratory analysis.

Dataset was sorted using the lowest q-values along false discovery rate (one-way ANOVA, post-hoc Tukey's HSD test and FDR Benjamini and Hochberg procedure) and the top 25 lipid species displaying the lowest q-values were ranked and used to create the heatmap (Figure 20). The top 25 list included five MGDG species, one DGDG, two SQDG species, four PC, one LPG, one LPE, one PE, eight DGTS species, and two MGTS species. The dendogram showed the separation of the nine locations (Figure 20). The first level of separation was evidenced between specimens from RAv and SE and the remaining origins. The second level of separation distinguished *Ulva* species from RAv, SE, and RP from the six remaining groups. Remaining groups were differentiated in six clusters in the third and fourth levels of separation. A new PCA considering these top 25 lipid species was performed and a new grouping was plotted (Figure 21). The eigenvalues of the PC1 plus PC2 increased, explaining now 67% of

total variance of the observations. Overall, a set of 25 site-specific molecular lipid species provide a unique lipidomic signature for authentication and geographic origin certification of *Ulva* species.

Results showed significant differences in the lipidomic profile displayed by *Ulva* spp. originating from different locations, namely due to different levels of polyunsaturated betaine lipids and galactolipids; saturated betaine lipids and sulfolipids; and some phospholipid species.

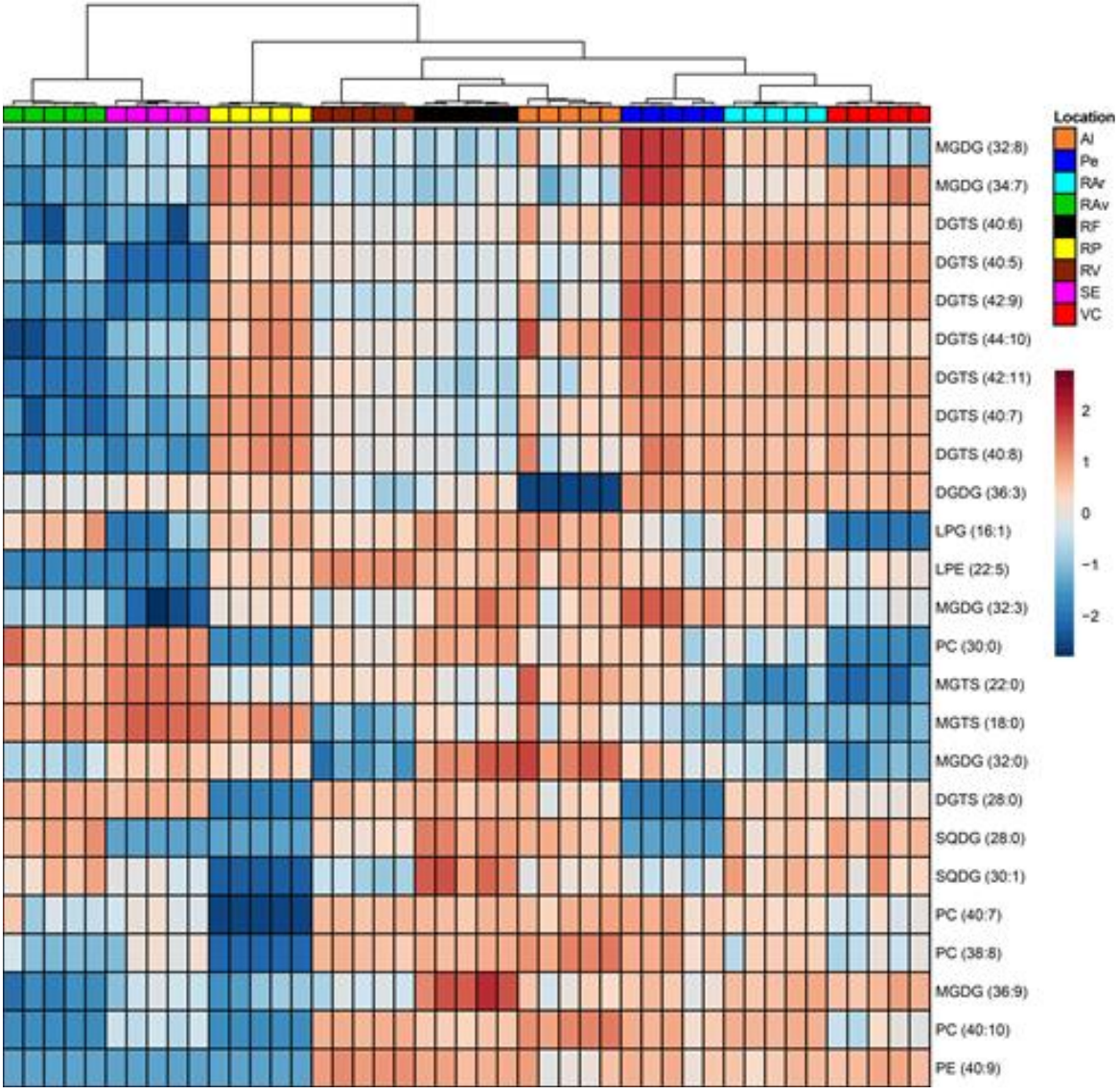


Figure 20. Hierarchical clustering heat map of lipid species data. Levels of normalized peak area are shown on the color scale, with numbers indicating the fold difference from the mean. The clustering of the sample groups is represented by the dendrogram of the top 25 lipid species displaying the lowest Tukey's HSD test q-values.

Labels of the sites are according to the notation: Albufeira (Al), Peniche (Pe), Ria Arousa (RAr), Ria de Aveiro (RAv), Ria Formosa (RF), Ria de Pontevedra (RP), Ria de Vigo (RV), Sado Estuary (SE), and Viana do Castelo (VC). Albufeira (Al), Peniche (Pe), Ria Arousa (RAr), Ria de Aveiro (RAv), Ria Formosa (RF), Ria de Pontevedra (RP), Ria de Vigo (RV), Sado Estuary (SE), and Viana do Castelo (VC). Labels of lipid species are according to the notation: AAAA (C:N), (AAAA, lipid class; C, total carbon atoms; N, total double bonds of fatty acid substituents).

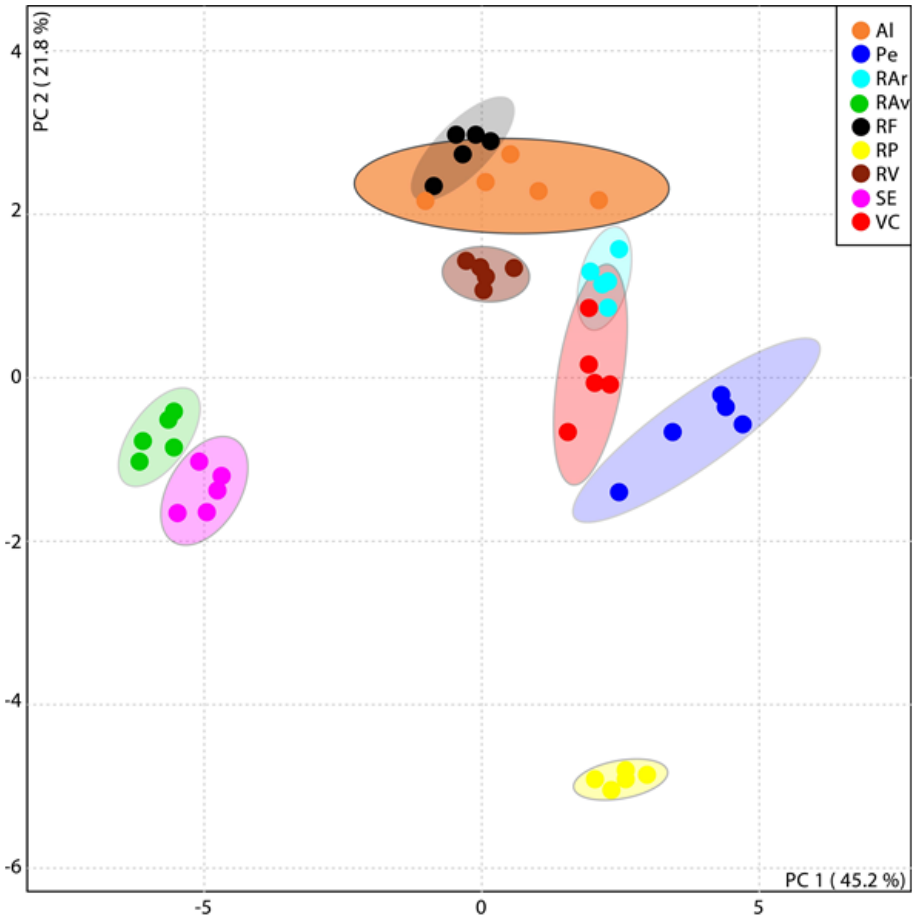


Figure 21. Principal component analysis (PCA) score plot of the top 25 lipid species displaying the lowest Tukey's HSD test q-values.
Labels of the sites are according to the notation: Albufeira (Al), Peniche (Pe), Ria Arousa (RAr), Ria de Aveiro (RAv), Ria Formosa (RF), Ria de Pontevedra (RP), Ria de Vigo (RV), Sado Estuary (SE), and Viana do Castelo (VC).

The present study found evidence supporting that site-specific lipid molecular species contributed to the reliable allocation of geographic origin of *Ulva* species. Twenty-five lipid species were highlighted as responding to site-specific conditions. This exploratory analysis showed a remarkable phenotypic plasticity of *Ulva* species lipidome and provided new insights into the relevant impact of environmental conditions on the response of cell membrane lipids. This knowledge encourages further investigation into the lipidome plasticity of seaweeds in general and *Ulva* spp. in particular, namely the effect of seasonal and interannual shifts in abiotic parameters, of culture conditions when employing land-based approaches, as well as larger scales of geographical variation (e.g., latitudinal clines). The knowledge of natural variation of *Ulva* spp. lipid composition holds potential for traceability purposes and strain selection.

## 2.4. Performance assessment of local *Ulva* strains (by CIIMAR)

From the *Ulva* biobank that is kept at CIIMAR, some strains were used to assess the effect of different light wavelengths on growth, sporulation, photosynthetic activity, pigments and antioxidant activity. Strains were collected at Belinho-Mar (-41.59113ºN; -8.80576°W) rocky shore, located in the northwest coast of Portugal, and maintained in f/2 medium, at 16 ± 1 ºC, using as source of light fluorescent biolux lamps with an intensity of 50 $\mu mol_{photon}.m^{-2}.s^{-1}$ and light/dark cycles of 12:12 h. A quick and simple experimental method was implemented, using circles of *Ulva* spp. thali with ca. 3,14 $cm^2$. Three monochromatic LED, blue (B), red (R) and green (G) were tested, as well as a polychromatic cold white (W) LED.

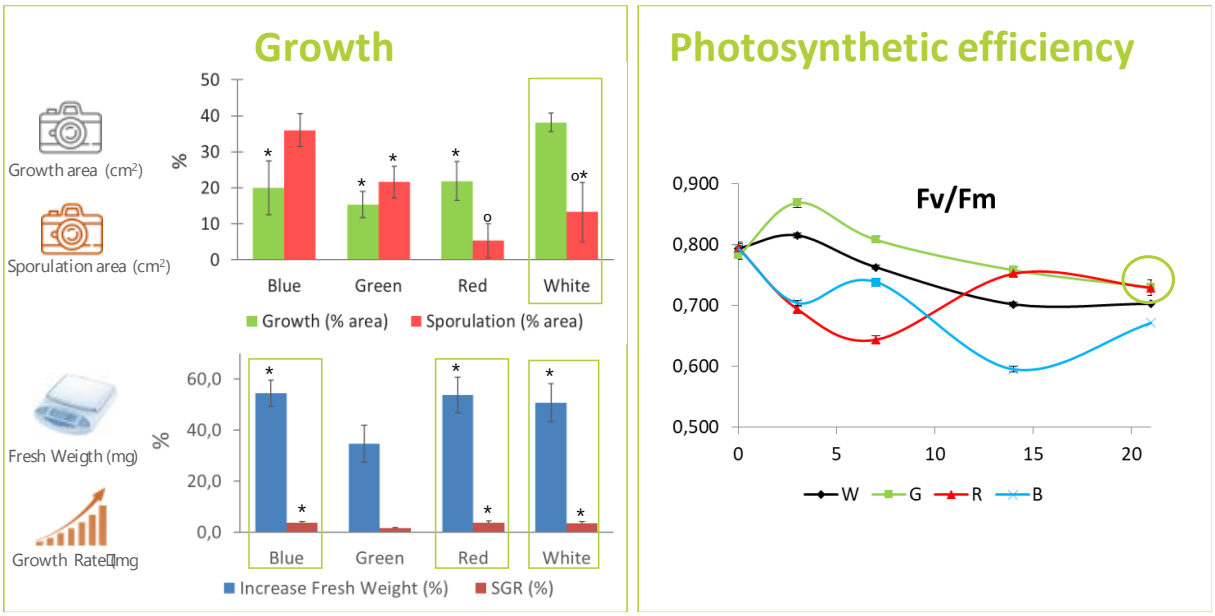


Figure 22. Growth (% area), increase in fresh weight (%), specific growth rate (SGR in %), sporulation (% area) and photosynthetic efficiency of *Ulva* strains in response to different light wavelengths. Bars with the same superscript symbol are not significantly different.

Results revealed that white light yielded the best results in terms of growth rate and no statistical differences were observed in growth under G, R and B. However, under G, quicker stabilization of photosynthesis rate was observed (Fig. 20), as well as the highest content in pigments, which was reflected on its bioactivity particularly on $ABTS^{+\bullet}$ assay. Also, R and W light quality seems to produce antioxidant compounds particularly against the radicals $O_2^{\bullet-}$ and $^{\bullet}NO^{-}$ (Fig. 21). Red light also seems to be beneficial in reducing sporulation and blue light in inducting fertility as it has been show for plant (Fankhauser and Chory, 1997) or other algae such as *S. latissima* (Lüning and Dring, 1975).

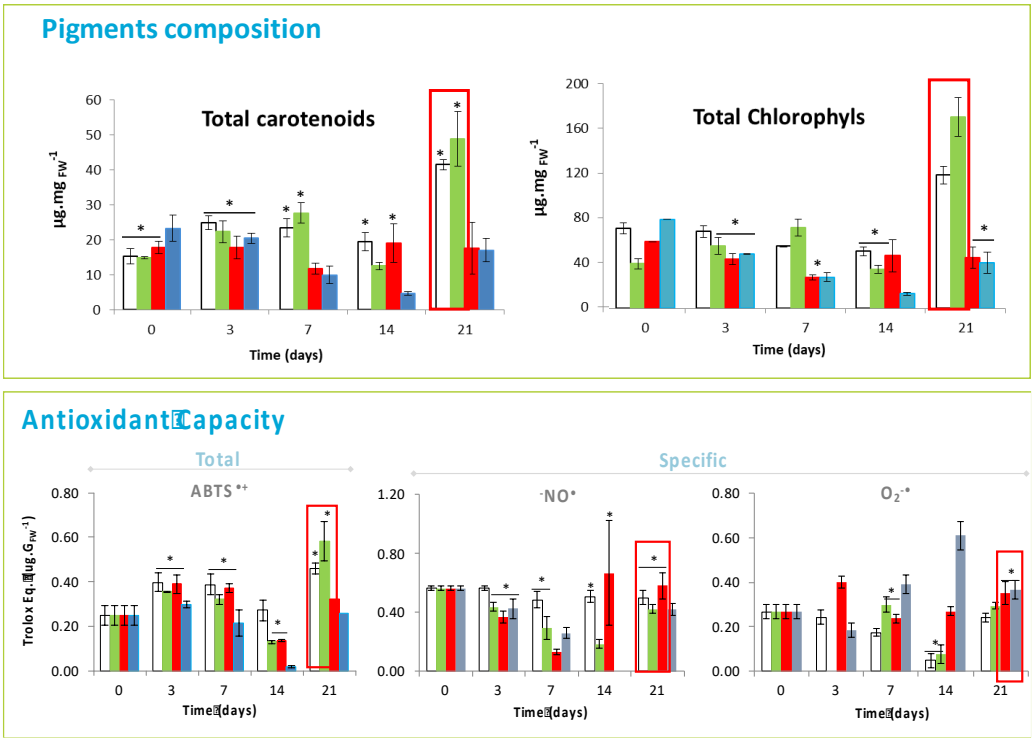


Figure 23. Pigment composition (top) and antioxidant capacity (bottom) of *Ulva* strains in response to different light wavelengths.
Bars with the same superscript symbol are not significantly different.

To assess if the effects of light quality are restricted to *Ulva* from Belinho, other *Ulva* strains collected from Matosinhos (41.175879°N; -8.693208°W) and Amorosa (41.641630°N; -8.823723°N), and phenotypically different, were tested under blue (B), red (R), green (G), and white (W) lights and resuts of growth (in flat circles and freely), sporulation, and biochemical profile were compared to growth under fluorescent light Biolux (F) (Fig. 22) Preliminary results indicate that the different *Ulva* strains had different growth responses for each light quality tested. Due to the Covid-19 lockdown, the biochemical assays were paused and will be returned as soon as possible.

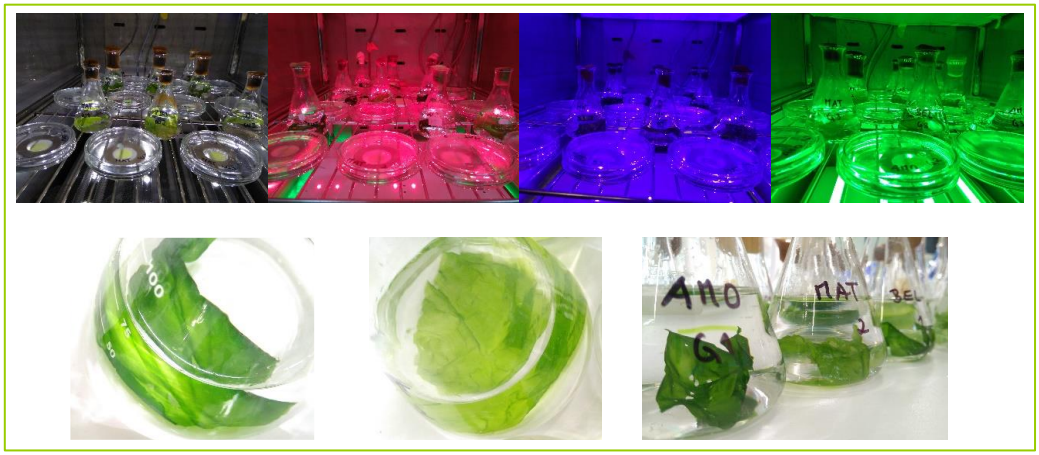

Figure 24. Trials assessing the effects of light quality on growth, sporulation and biochemical profile using phenotypically different *Ulva* strains collected in Belinho, Matosinhos and Amorosa rocky shores.

## 2.5. Performance assessment of *Ulva* strains (by WUR, link with WP3)

*Ulva* strains were collected in 2017 (5), 2018 (10) and 2019 (13) along the coast of the Eastern Scheldt (Netherlands), and analyzed for **productivity** and **chemical composition**, using a land-based cultivation system of 600 L containers (Figure 25 A). Fresh seawater was replenished ~5 times a day. Both in 2017 (solid lines) and 2018 (dashed lines) productivity varied greatly between strains from max. 600 to nearly zero kg fresh weight per ha per day (Figure 25 B). The two best performing 2017 strains (yellow and green) were biobanked over the winter period and cultivated again in 2018 (dashed lines) the "yellow" strain showed no growth and only survived the growing season. The 2019 strains initially showed poor growth and almost all strains died during the extremely hot summer period (>40°C).

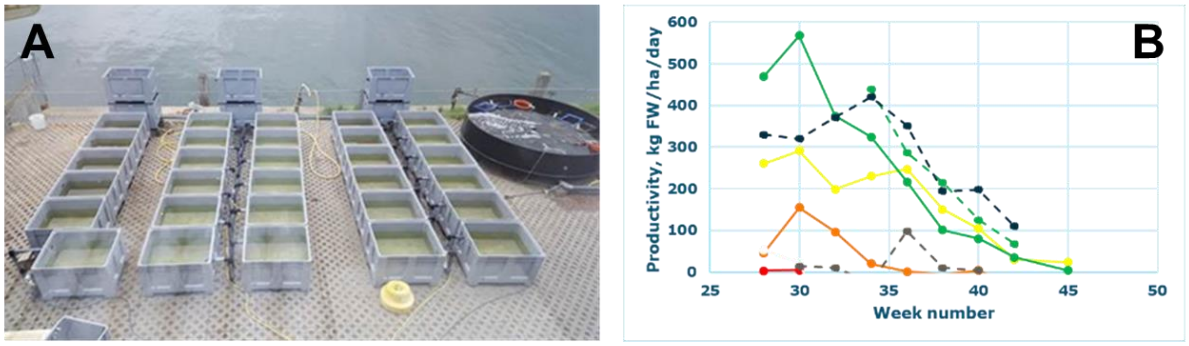


Figure 25. An *Ulva* land-based cultivation system (WUR) B. *Ulva* selected strains productivity in 2017 and 2018.

Crude protein concentrations strongly increased over the growing season, whereas that of starch strongly declined (Figure 26). No trend was observed in ash, dietary fiber or lipid content (data not show).

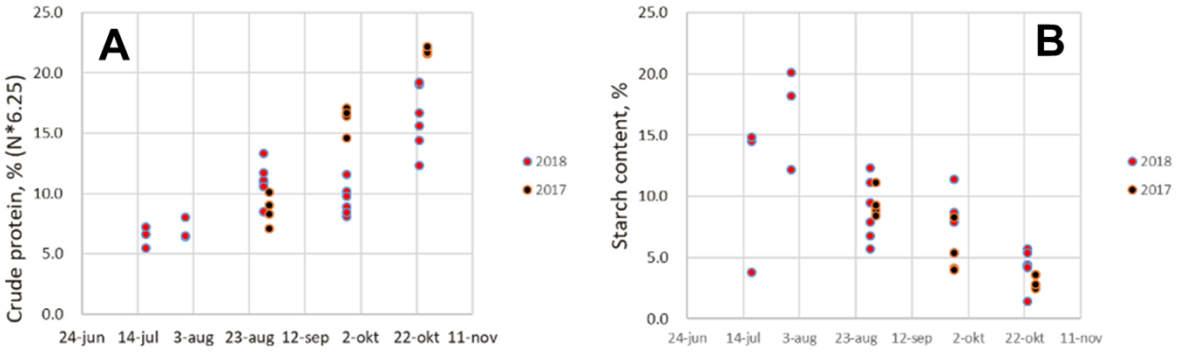


Figure 26. *Ulva* spp. proteins and starch concentration evolution in 2017 and 2018.

Protein content of food products is generally calculated as N-concentration times 6.25 (Mariotti et al., 2008). We analyzed all essential and non-essential amino acids and calculated true protein as their sum, corrected for $H_2O$ loss in peptide bonding and we observed a constant

factor of ~4.6-5 irrespective of strain and season, suggesting that N-concentration can safely be used as an indicator of true protein content for *Ulva* spp. (Figure 27). In all cases the amino acid composition met the requirements for humans as set by the FAO (Joint, 2007) and more or less equaled to microalgae and soy (Gorissen et al., 2018).

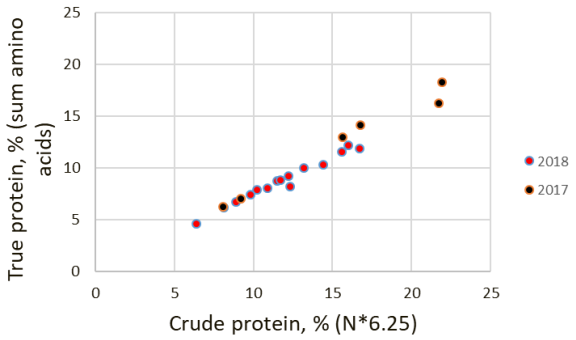


Figure 27. Linear correlation between crude and true protein content in *Ulva* samples in 2017 and 2018

Protein content strongly increased from summer to autumn (Figure 26 A), and this increase corresponded with an increased N-concentration in Eastern Scheldt water. In 2019, we conducted a nitrogen addition experiment to further check if protein concentration can be held constant over the season in land-based cultivation systems. Due to the extreme summer of 2019 we could not finish the experiment. We intend to perform a similar experiment in 2020.

To summarize, large variation between strains in productivity was observed and protein and starch content varied by factor of three over the growing season regardeless of the strain, warranting a careful search for high productive, high quality strains.

## 2.6. Genome wide association studies (GWAS) on *Ulva* spp. (by NUIG)

*Ulva* is increasingly grown in an aquaculture context, for food, feed, production of bioactive compounds and in Integrated Multi-Trophic Aquaculture (Adrien et al., 2019; Amosu et al., 2016; Ghaderiardakani et al., 2019; Magnusson et al., 2019). Despite the strong interest in industrialising *Ulva* production, the strains grown in the aquaculture systems have not yet been selected for specific uses, and largely rely on local strains collected in the vicinity of the farming site (Silva et al., 2015). In this context, strain selection through high throughput phenotyping coupled with genomic selection (i.e. Genome Wide Association Study) to identify genetic markers associated with high yield(s) of interest could potentially lead to significant increases in farming systems outputs.

### 2.6.1. High-throughput, laboratory-based phenotyping

Samples that survived the transport and the growth conditions in NUIG were phenotyped according to (Fort et al., 2019) using a custom-made phenotyping platform. Data obtained from all strains include growth, physiological and metabolic parameters. The list of phenotypes is shown in Table 7. Currently 22 traits are included in the phenotyping, but additional metabolic analysis can be performed.

Table 7. List of phenotypes measured for *Ulva* strain phenotyping.

| Trait | Abbreviation | Trait type | Unit |
|---|---|---|---|
| Day Specific Growth Rate | Day SGR | Growth | %.day$^{-1}$ |
| Night Specific Growth Rate | Night SGR | Growth | %.day$^{-1}$ |
| Daily Specific Growth Rate | Daily SGR | Growth | %.day$^{-1}$ |
| Relative Growth Rate | RGR | Growth | %.day$^{-1}$ |
| Fresh Weight | FW | Growth | mg |
| Dry Weight | DW | Growth | mg |
| Net Assimilation Rate | NAR | Physiological | mg mm$^{-2}$ day$^{-1}$ |
| Specific Leaf Area | SLA | Physiological | mm$^2$.mg$^{-1}$ |
| Water content | WC | Physiological | % |
| Starch | | Metabolic | µmol.g DW$^{-1}$ |
| Protein | | Metabolic | mg.g DW$^{-1}$ |
| Amino Acids | AA | Metabolic | µmol.g DW$^{-1}$ |
| Chlorophyll a | Chla | Metabolic | mg.g DW$^{-1}$ |
| Chlorophyll b | Chlb | Metabolic | mg.g DW$^{-1}$ |
| Carotenoids | Car | Metabolic | mg.g DW$^{-1}$ |
| Nitrates | $NO_3$ | Metabolic | $NO_3^-$-N mg.g DW$^{-1}$ |
| Nitrite | $NO_2$ | Metabolic | $NO_2^-$-N mg.g DW$^{-1}$ |
| Glucose | Glc | Metabolic | µmol.g DW$^{-1}$ |

| | | | |
|---|---|---|---|
| Fructose | Fru | Metabolic | µmol.g $DW^{-1}$ |
| Sucrose | Suc | Metabolic | µmol.g $DW^{-1}$ |
| Starch turnover | | Metabolic | µmol.g $DW^{-1}.night^{-1}$ |
| Nitrate turnover | | Metabolic | µmol.g $DW^{-1}.night^{-1}$ |

To date, 220 *Ulva* strains have been phenotyped and a subset of the data has been published (Fort et al., 2019; Fort et al., 2020). Overall, our data demonstrates the potential for strain selection to increase yield(s), since large variations were observed for all traits measured. For example, biomass accumulation (RGR) showed a ~four-fold variation between strains, while protein accumulation can vary with a factor of five (Figure 28). Hence, selecting strains prior to their use for aquaculture is likely to lead to strong yields improvement.

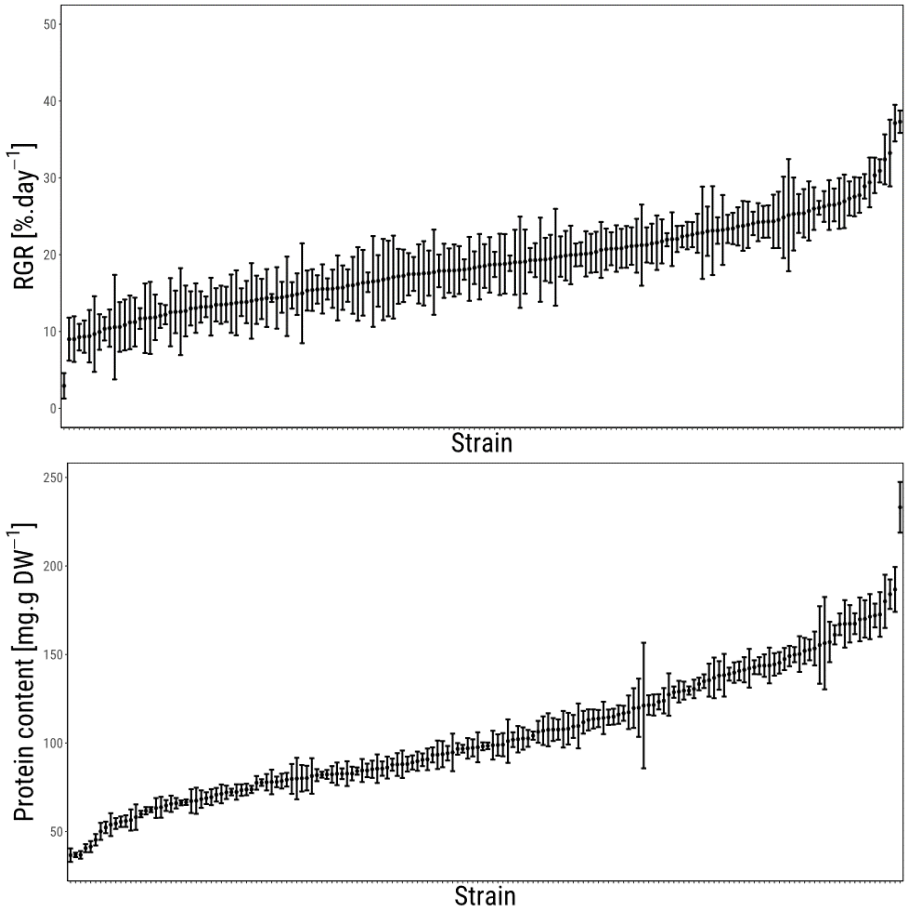


Figure 28. Relative Growth Rate (top) and Protein content (bottom) of the fully phenotyped *Ulva* strains. Data represent the mean ± standard deviation of eight biological replicates.

## 2.6.2. Genotyping *Ulva* spp.

Genotyping of *Ulva* strains for the GWAS analysis was performed using Whole Genome Sequencing (WGS) (Illumina 150 bp Paired End). Genotyping has been carried out for 110 to date, using DNA extracted with a protocol developed at NUIG (Fort et al., 2018). In parallel, a single strain (CLO4, from Ireland), has been genotyped using Oxford Nanopore MinION long reads technology. We found surprisingly large genetic diversity between *Ulva* species, despite being morphologically similar. So far, our analysis focused on the organellar genomes to precisely characterise the species of each strain in our dataset (Fort et al., under review) (see Figure 29 for the strains genotyped, their location and the relative abundance of *Ulva* species detected).

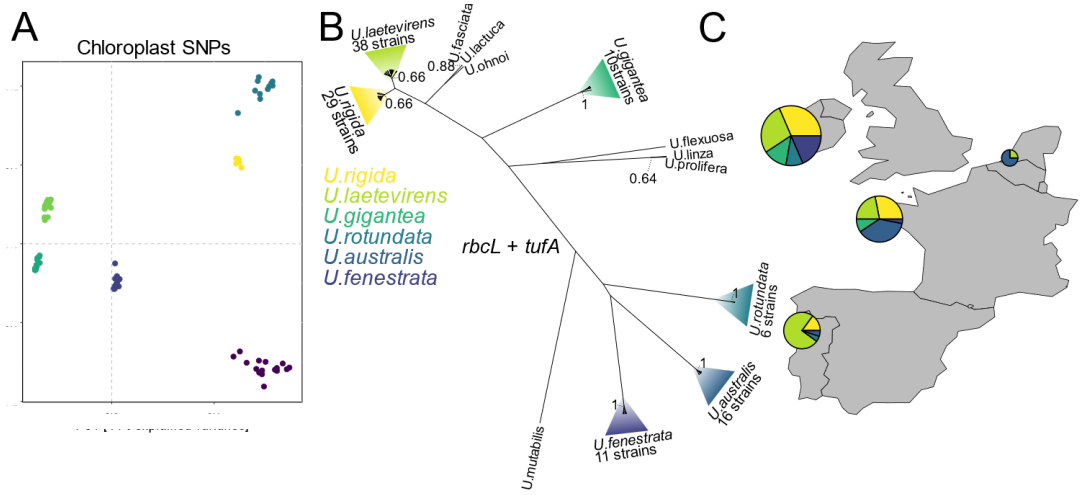


Figure 29. *Ulva* samples genotyped to date.
A) Clustering of strains based on their chloroplast genome sequence. Principal Component Analysis (PC1 and PC4) of SNP data for each strain compared to a nanopore assembly of the chloroplast genome of strain U41. Colours represent the six clusters found. B) Phylogenetic tree of the 110 sampled individuals based on *rbcL* and *tufA* concatenated sequences under a Yule model. Numbers represent support for species-specific clusters. Colours represent the assigned species to the cluster. C) Sampling locations and relative abundance of each laminar *Ulva* species. (Fort et al., under review)

Interestingly, we found only one case of inter-species hybridization between the *Ulva* strains genotyped, indicating that laminar *Ulva* species are generally reproductively isolated, even in areas were four or five species are present. The remainder of the phenotyped strains will be sequenced in the first half of 2020.

Identification of laminar *Ulva* species based on morphology has proven difficult over the years. Indeed, while species have been shown to display different characteristics in some studies, the possible plasticity of those characteristics render identification based solely on morphology hazardous. Hence, molecular identification represents the method of choice for laminar *Ulva*. However, molecular identification relies on the sequencing of PCR products of barcode genes (typically *rbcL* and *tufA* in *Ulva*). Such sequencing is relatively costly and time-consuming when used on hundreds of *Ulva* strains, in the case of a strain selection programme where a single laminar *Ulva* species is desirable. Indeed, selecting individuals belonging to a given

species requires i) PCR amplification, ii) PCR products purification, iii) sequencing of PCR products and iv) species identification based on the sequencing results.

When considering a breeding programme with thousands of samples, a faster/cheaper approach is desirable. One such approach is the detection of specific SNPs associated with a given species by Cleaved Amplified Polymorphic Sequences (CAPS) assay. CAPS assay uses restriction enzymes digestion on PCR products to detect the presence (or absence) of specific SNPs in the samples (Fort and *al*., in prep). We designed a CAPS assay to discriminate laminar *Ulva* species based on species-specific SNPs in the ITS1 sequence (part of the 45S rRNA genes). For each of the six species (*U. laetevirens, U. rigida, U. gigantea, U. rotundata, U. australis* and *U. fenestrata*) in our dataset, we identified restriction digestion sites containing SNPs present in all of the individuals for a given species (Figure 29A). We selected specifically restriction sites for DNA methylation-insensitive enzymes to ensure complete digestion of the PCR product, regardless of the methylation status of the DNA. For example, all 37 of *U. laetevirens* individuals possess a unique restriction site for *Bfa*I in the amplified fragment of the ITS1, making it simple to discriminate *U. laetevirens* sequences from sequences of five other species after PCR product digestion with *Bfa*I.

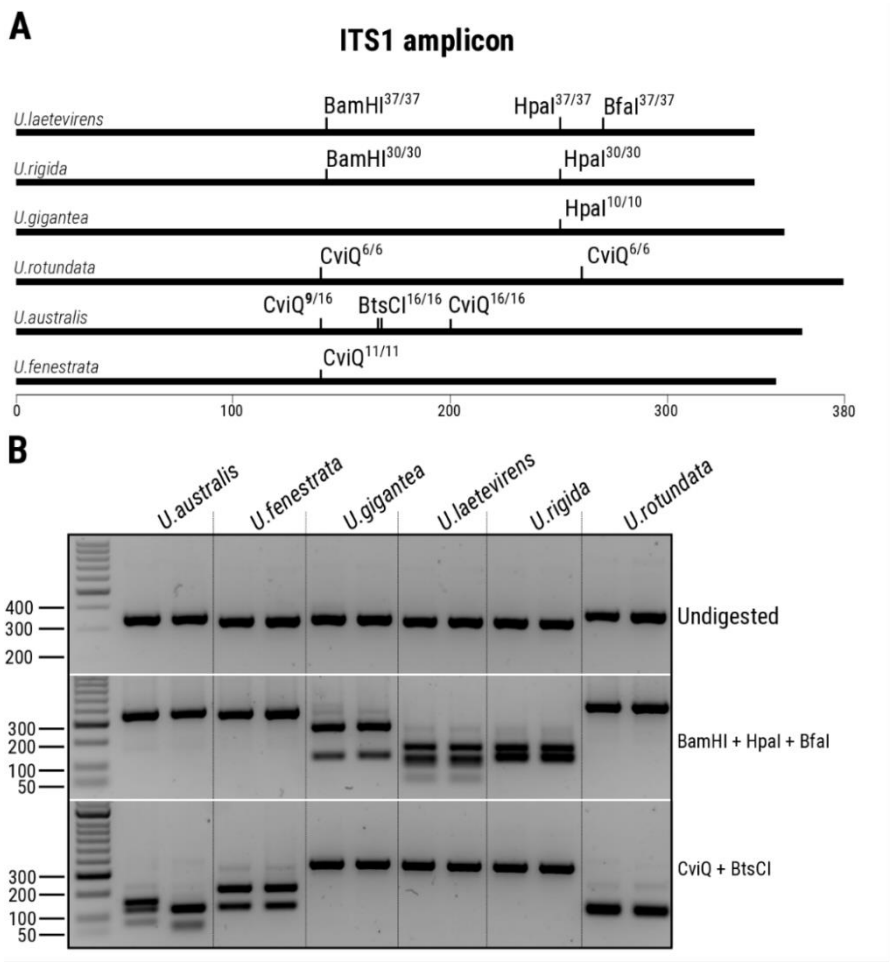


Figure 30. Novel CAPS assay for *Ulva* species identification.
A) ITS1 amplicon used in the CAPS assay. Restriction sites for the enzymes used, as well as the relative presence of the site among all the strains genotyped to date are indicated. B) Results of digestion of the ITS1 amplicons with the enzymatic mixtures. Two individuals for each species have been used.

Our assay uses two different enzymes mixtures that can be employed to quickly select strains belonging to either of the six species. The *Bam*HI/*Hpa*I/*Bfa*I mixture discriminates between *U. laetevirens*, *U. rigida* and *U. gigantea* DNA samples, with the complete digestion of the ITS1 PCR product and generation of a specific band pattern for each species (Figure 30B). *U. gigantea*, *U. australis* and *U. fenestrata* samples will not be digested using this mixture. For those species, another enzyme cocktail can be used (*Cvi*Q/*Bts*CI), which will completely digest the ITS1 PCR products and again release a specific band pattern that can be easily distinguished between those three species (Figure 30B). Only *U. australis* showed a restriction site polymorphism within the 16 individuals of this species in our dataset, with the first *Cvi*Q restriction site being present in only 9 out of the 16 individuals. Nonetheless, this polymorphism creates a specific band pattern that is unique compared with samples from the 5 other species (first two samples of Figure 30B). Hybrids, if present, can similarly be detected: we used our assay on the *U. laetevirens/U. rigida* hybrid identified by WGS, and were able to classify it as a hybrid (Figure 31). Hence, our CAPS assay can be used to accurately, cheaply and quickly select individuals from a species of interest prior to strain selection, or indeed to assess the distribution of species within areas. This assay could be validated and extended to other laminar species once their complete 4.5S / ITS1 sequences become available.

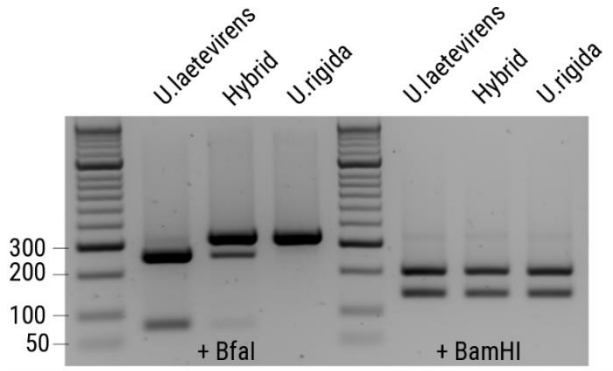


Figure 31. Detection of inter-species hybrids using the CAPS assay.

The identification of species within genus *Ulva* has long been recognized as an extremely challenging task, with these green seaweeds displaying a remarkable level of morphological plasticity. So far, strains sent by UAVR/ALGAplus (R1-R17) have been analysed for genotyping. Strains described in Table 6 and collected from the wild were termed as *Ulva* species. Freeze-dried fragments of *Ulva* spp. have been preserved for future species identification once the taxonomic issues of these genus are clarified and robust DNA barcoding protocols are made available for family Ulvaceae.

### 2.6.3. Biobanking and cryopreservation of *Ulva* spp.

All WP2 partners are involved with the development of a cryopreservation protocol for *Ulva* spp. Our initial findings are encouraging, with generally good recovery rates for the cryopreserved material, either through the direct regeneration of the thallus or the creation of viable spores out of the cryopreserved sample. 46 strains are currently in NUIG cryo-collection. Freeze dried material for all 220 strains used by NUIG for phenotyping are also in

storage. All strains collected during 2018 and 2019 by UAVR/ALGAplus (Table 3) are maintained in ALGAplus facilities (laboratory).

As an example, WUR collaborated in the biobanking and cryopreservation of *Ulva* spp.

**Biobanking methods**

Once high productive, high quality strains have been identified, strains need to be preserved over the years, which is of special relevance for commercial large scale seaweed cultivation. Around 70 *Ulva* "populations" were sampled in 2018-2019 in the Eastern Scheldt (Netherlands) and of each population 1 healthy looking thallus was stored in 600 ml cup glasses with the following specifications:

- long-term storage for 2.5 – 3.5 months in filtered seawater (with nutrients added) at 12 °C, 12 hour light/12 hour dark, PPFD 35-50 µmol $m^{-2}$ $s^{-1}$, no aeration.
- long-term storage for 3 months up to 2 years in filtered seawater (no nutrients added) at 6 °C, 7 hour light/17 hour dark, PPFD ~ 4 µmol $m^{-2}$ $s^{-1}$, +/- aeration.
- long-term storage for 3 months in filtered seawater (no nutrients added) at 0-4°C.

Using the first method almost all populations started to sporulate within several months and is therefore not recommended.
Following the second method, we were able to store *Ulva* populations for up to 2 years, but visual inspection showed that after one year 50% of of the populations had died and after two years 75%.
As this method gave promising results, we decided not to pursue the test with the third method. However, it should be noted that after three months of storage in the dark at 0-4 $^{o}$C, thalli visually looked healthy.

We conclude that the second method could be used for biobanking populations that are used for scientific experiments within say one year. For commercial purposes biobanking of seaweed is a laborious way of preserving high quality material, and it is suggested to look for other ways to preserve specific strains.

**Re-growth after biobanking**

Re-growth after biobanking following the chosen method was tested in the second half of 2019. Populations had been biobanked for 4 to 11 months, and the following environmental conditions were applied to test re-growth capacity: 20°C, 17 h light/ 7 h dark cycle and a PPFD 90 to 110 µmol $m^{-2}s^{-1}$. The aerated nutrient solution was renewed once every 1-4 weeks. In general all populations showed remarkable re-growth the first weeks after biobanking with relative growth rates of > 300 mg $g^{-1}$ $day^{-1}$. In most cases growth ceased after several weeks and material started sporulating. In conclusion, biobanking according to the chosen method was succesfull, but environmental re-growth conditions need to be optimized further.

**Induction of sporulation after biobanking**

To consistently cultivate *Ulva* spp., sufficient seedstock is needed to provide the preferred *Ulva* strain or species that can subsequently be grown and then harvested. To produce this seedstock, a reliable method is needed to induce the sporulation of *Ulva*. The formation and release of zoospores and gametes is regulated by three factors, Sporulation Inhibitor 1 (SI-1), Sporulation Inhibitor 2 (SI-2) and Swarming Inhibitor (SWI). SI-1 is present in the medium around the thallus and in the blade cell walls and inhibits the formation of gametangia. SI-2

occurs between the two cell layers and inhibits the formation of gametangia. Only when the levels of both SI-1 and SI-2 are low enough, the formation of gametangia can occur. SWI is synthesized and released in the medium during the formation of the gametangia and inhibits the release of the gametes. This is to make the release of gametes simultaneous and not to occur at the wrong moment such as e.g. a low tide. Furthermore, specific environmental factors, like temperature and nutrient concentration may induce sporulation systematically. In 2020 we started testing two sporulation induction protocols: 1) induction of sporulation by increasing the nutrient concentration, and 2) induction of sporulation via removal of the extracellular inhibitors SI-1, SI-2 and SWI by washing and fragmenting the thallus. Protocols 1 and 2 were tested for several populations that were biobanked for several weeks up to 9 months according to chosen biobanking method as described above.

Preliminary experiments showed positive results for protocol 1. Irrespective of strains used, material sporulated after 4-5 days, and protocol 2 gave mixed results. Both protocols will be further tested after Covid-19.

**Cryo-preservation**

Cryo-preservation could be a valuable alternative for biobanking as it requires far less maintenance and labor during storage. NUIG developed a cryo-preservation protocol which was based on the one described in (Lee and Nam, 2016). SAMS and WUR successfully tested the NUIG protocol with slight modifications. As an example, WUR successfully cryo-preserved three *Ulva* populations for two weeks at -196°C and were able to re-grow the cryo-preserved material of two populations (Figure 32).

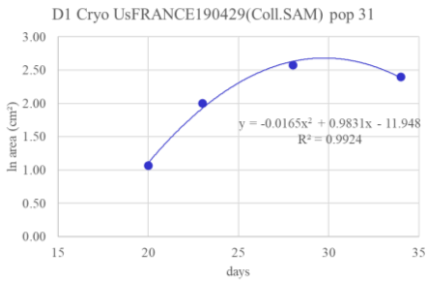


Figure 32. Increase in leaf area of *Ulva* population D1 UsFRANCE190429(Coll.SAM) after recovery of cryopreservation -196°C.

As in the case of the biobanked material, the growth ceased after several weeks when *Ulva* started sporulating. The spores were able to grow to small thallus with a holdfast (Figure 33). In 2020, WUR hope to start testing biological material that has been cryo-preserved for longer periods and optimize the growth and sporulation conditions post cryo-preservation.

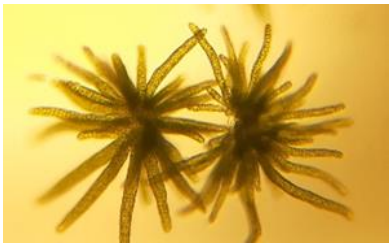

Figure 33. Germinating *Ulva* spp. several weeks after resumption of growth post cryo-preservation.

# 3. Outputs

Up to now,6 peer-reviewed manuscripts have already been published or submitted under the umbrella of this deliverable. Information related those publications can be found on the GENIALG website "Publications" page https://genialgproject.eu/results/publications/.

1. **Magnetic beads, a particularly effective novel method for extraction of NGS-ready DNA from macroalgae (Fort et al., 2018)**

GENIALG partner: NUIG
Antoine Fort, Michael D. Guiry, Ronan Sulpice
Published in Algal Research 2018
https://doi.org/10.1016/j.algal.2018.04.015

2. **Underpinning the Development of Seaweed Biotechnology: Cryopreservation of Brown Algae (*Saccharina* latissima) Gametophytes (Visch et al., 2019)**

GENIALG partner: SAMS
Published in Biopreservation and Biobanking 2019
https://doi.org/10.1089/bio.2018.0147

3. **Extensive variations in diurnal growth patterns and metabolism among *Ulva* spp. strains (Fort et al., 2019)**

GENIALG partner: NUIG
Antoine Fort, Morgane Lebrault, Margot Allaire, Alberto A. Esteves-Ferreira, Marcus McHale, Francesca Lopez, Jose M. Fariñas-Franco, Saleh Alseekh, Alisdair R. Fernie, and Ronan Sulpice
Published in Plant physiology 2019
https://doi.org/10.1104/pp.18.01513

4. **Green tides select for fast expanding *Ulva* strains (Fort et al., 2020)**

GENIALG partner: NUIG
Antoine Fort, Conor Mannion, Jose M. Fariñas-Franco, Ronan Sulpice
Published in Science of The Total Environment 2020
https://doi.org/10.1016/j.scitotenv.2019.134337

5. **Site-specific lipidomic signatures of sea lettuce (*Ulva* spp., Chlorophyta) hold the potential to trace their geographic origin (da Costa et al., 2020)**

GENIALG partner: UAVR, ALGAplus
Elisabete da Costa, Fernando Ricardo, Tânia Melo, Renato Mamede, Maria H. Abreu, Pedro Domingues, M. Rosário Domingues,, Ricardo Calado
Published in Biomolecules 2020
https://doi.org/10.3390/biom10030489

6. **Laminar *Ulva* species show considerable genetic diversity among European species, and the rare occurrence of inter-specific hybrids. (Fort et al., under review)**

GENIALG partner: NUIG
Antoine Fort, Marcus McHale, Kevin Cascella, Philippe Potin, Björn Usadel, Michael D Guiry, Ronan Sulpice
Submitted

# 4. References


Adrien, A., A. Bonnet, D. Dufour, S. Baudouin, T. Maugard, and N. Bridiau. 2019. Anticoagulant activity of sulfated ulvan isolated from the green macroalga Ulva rigida. *Marine drugs*. 17:291.

Amosu, A., D. Robertson-Andersson, E. Kean, G. Maneveldt, and L. Cyster. 2016. Biofiltering and uptake of dissolved nutrients by Ulva armoricana (Chlorophyta) in a land-based aquaculture system. *Int. J. Agri. Biology*. 18:298-304.

Avia, K., S.M. Coelho, G.J. Montecinos, A. Cormier, F. Lerck, S. Mauger, S. Faugeron, M. Valero, J.M. Cock, and P. Boudry. 2017. High-density genetic map and identification of QTLs for responses to temperature and salinity stresses in the model brown alga Ectocarpus. *Sci Rep*. 7:43241.

Badis, Y., T.A. Klochkova, M. Strittmatter, A. Garvetto, P. Murúa, J.C. Sanderson, G.H. Kim, and C.M. Gachon. 2019. Novel species of the oomycete Olpidiopsis potentially threaten European red algal cultivation. *J Appl Phycol*. 31:1239-1250.

Bolton, J., D. Robertson-Andersson, D. Shuuluka, and L. Kandjengo. 2009. Growing Ulva (Chlorophyta) in integrated systems as a commercial crop for abalone feed in South Africa: a SWOT analysis. *Journal of Applied Phycology*. 21:575-583.

Brachi, B., G.P. Morris, and J.O. Borevitz. 2011. Genome-wide association studies in plants: the missing heritability is in the field. *Genome biology*. 12:232.

Breton, T.S., J.C. Nettleton, B. O'Connell, and M. Bertocci. 2018. Fine-scale population genetic structure of sugar kelp, Saccharina latissima (Laminariales, Phaeophyceae), in eastern Maine, USA. *Phycologia*. 57:32-40.

Calmes, B., M. Strittmatter, B. Jacquemin, M.-M. Perrineau, C. Rousseau, Y. Badis, J.M. Cock, C. Destombe, M. Valero, and C.M. Gachon. 2020. Parallelisable non-invasive biomass, fitness and growth measurement of macroalgae and other protists with nephelometry. *Algal Research*. 46:101762.

da Costa, E., F. Ricardo, T. Melo, R. Mamede, M.H. Abreu, P. Domingues, M.R. Domingues, and R. Calado. 2020. Site-Specific Lipidomic Signatures of Sea Lettuce (Ulva spp., Chlorophyta) Hold the Potential to Trace Their Geographic Origin. *Biomolecules*. 10:489.

Derevnina, L., B. Petre, R. Kellner, Y.F. Dagdas, M.N. Sarowar, A. Giannakopoulou, J.C. De la Concepcion, A. Chaparro-Garcia, H.G. Pennington, P. van West, and S. Kamoun. 2016. Emerging oomycete threats to plants and animals. *Philos Trans R Soc Lond B Biol Sci*. 371.

Durrant, H.M., C.P. Burridge, B.P. Kelaher, N.S. Barrett, G.J. Edgar, and M.A. Coleman. 2014. Implications of macroalgal isolation by distance for networks of marine protected areas. *Conservation biology*. 28:438-445.

Evankow, A., H. Christie, K. Hancke, A.K. Brysting, C. Junge, S. Fredriksen, and J. Thaulow. 2019. Genetic heterogeneity of two bioeconomically important kelp species along the Norwegian coast. *Conserv Genet*. 20:615-628.

Fankhauser, C., and J. Chory. 1997. Light control of plant development. *Annual review of cell and developmental biology*. 13:203-229.

FAO. 2018. The State of World Fisheries and Aquaculture 2018 - Meeting the sustainable development goals.

Fort, A., and *al*. in prep. Reassessment of laminar *Ulva* phylogeny and distribution across the European Coast.

Fort, A., M.D. Guiry, and R. Sulpice. 2018. Magnetic beads, a particularly effective novel method for extraction of NGS-ready DNA from macroalgae. *Algal research*. 32:308-313.

Fort, A., M. Lebrault, M. Allaire, A.A. Esteves-Ferreira, M. McHale, F. Lopez, J.M. Farinas-Franco, S. Alseekh, A.R. Fernie, and R. Sulpice. 2019. Extensive Variations in Diurnal Growth Patterns and Metabolism Among Ulva spp. Strains. *Plant Physiol*. 180:109-123.

Fort, A., C. Mannion, J.M. Farinas-Franco, and R. Sulpice. 2020. Green tides select for fast expanding Ulva strains. *Sci Total Environ*. 698:134337.

Fort, A., M. McHale, K. Cascella, P. Potin, B. Usadel, M. Guiry, and R. Sulpice. under review. Laminar Ulva species show considerable genetic diversity among european species, and the rare occurrence of inter-specific hybrids.

Gachon, C.M., M. Strittmatter, D.G. Muller, J. Kleinteich, and F.C. Kupper. 2009. Detection of differential host susceptibility to the marine oomycete pathogen Eurychasma dicksonii by real-time PCR: not all algae are equal. *Appl Environ Microbiol*. 75:322-328.

Ghaderiardakani, F., G. Califano, J.F. Mohr, M.H. Abreu, J.C. Coates, and T. Wichard. 2019. Analysis of algal growth-and morphogenesis-promoting factors in an integrated multi-trophic aquaculture system for farming Ulva spp. *Aquaculture Environment Interactions*. 11:375-391.

Gorissen, S.H., J.J. Crombag, J.M. Senden, W.H. Waterval, J. Bierau, L.B. Verdijk, and L.J. van Loon. 2018. Protein content and amino acid composition of commercially available plant-based protein isolates. *Amino acids*. 50:1685-1695.

Guzinski, J., S. Mauger, J.M. Cock, and M. Valero. 2016. Characterization of newly developed expressed sequence tag-derived microsatellite markers revealed low genetic diversity within and low connectivity between European Saccharina latissima populations. *J Appl Phycol*. 28:3057-3070.

Hayden, H.S., J. Blomster, C.A. Maggs, P.C. Silva, M.J. Stanhope, and J.R. Waaland. 2003. Linnaeus was right all along: Ulva and Enteromorpha are not distinct genera. *European journal of phycology*. 38:277-294.

Heesch, S., G.Y. Cho, A.F. Peters, G. Le Corguille, C. Falentin, G. Boutet, S. Coedel, C. Jubin, G. Samson, E. Corre, S.M. Coelho, and J.M. Cock. 2010. A sequence-tagged genetic map for the brown alga Ectocarpus siliculosus provides large-scale assembly of the genome sequence. *New Phytol*. 188:42-51.

Hughey, J.R., C.A. Maggs, F. Mineur, C. Jarvis, K.A. Miller, S.H. Shabaka, and P.W. Gabrielson. 2019. Genetic analysis of the Linnaean Ulva lactuca (Ulvales, Chlorophyta) holotype and related type specimens reveals name misapplications, unexpected origins, and new synonymies. *Journal of phycology*. 55:503-508.

Joint, W. 2007. Protein and amino acid requirements in human nutrition. *World health organization technical report series*:1.

Kamoun, S., O. Furzer, J.D. Jones, H.S. Judelson, G.S. Ali, R.J. Dalio, S.G. Roy, L. Schena, A. Zambounis, F. Panabieres, D. Cahill, M. Ruocco, A. Figueiredo, X.R. Chen, J. Hulvey, R. Stam, K. Lamour, M. Gijzen, B.M. Tyler, N.J. Grunwald, M.S. Mukhtar, D.F. Tome, M. Tor, G. Van Den Ackerveken, J. McDowell, F. Daayf, W.E. Fry, H. Lindqvist-Kreuze, H.J. Meijer, B. Petre, J. Ristaino, K. Yoshida, P.R. Birch, and F. Govers. 2015. The Top 10 oomycete pathogens in molecular plant pathology. *Mol Plant Pathol*. 16:413-434.

Khan, S., Y. Mao, D. Gao, S. Riaz, Z. Niaz, L. Tang, S. Khan, and D. Wang. 2018. Identification of proteins responding to pathogen-infection in the red alga Pyropia yezoensis using iTRAQ quantitative proteomics. *BMC Genomics*. 19:842.

Kim, G.H., K.-H. Moon, J.-Y. Kim, J. Shim, and T.A. Klochkova. 2014. A revaluation of algal diseases in Korean Pyropia (Porphyra) sea farms and their economic impact. *Algae*. 29:249.

Korte, A., and A. Farlow. 2013. The advantages and limitations of trait analysis with GWAS: a review. *Plant Methods*. 9:29.

Lee, H.W., J.C. Kang, and M.S. Kim. 2019. Taxonomy of Ulva causing blooms from Jeju Island, Korea with new species, U. pseudo-ohnoi sp. nov. (Ulvales, Chlorophyta). *ALGAE*. 34:253-266.

Lee, Y.N., and K.W. Nam. 2016. Cryopreservation of gametophytic thalli of Ulva prolifera (Ulvales, Chlorophyta) from Korea. *J Appl Phycol*. 28:1207-1213.

Liu, F., Z. Shao, H. Zhang, J. Liu, X. Wang, and D. Duan. 2010. QTL mapping for frond length and width in Laminaria japonica aresch (Laminarales, Phaeophyta) using AFLP and SSR markers. *Mar Biotechnol (NY)*. 12:386-394.

Liu, F., J. Yao, X. Wang, Z. Hu, and D. Duan. 2011. Identification of SCAR marker linking to longer frond length of Saccharina japonica (Laminariales, Phaeophyta) using bulked-segregant analysis. *J Appl Phycol*. 23:709-713.

Lopes, D., A.S. Moreira, F. Rey, E. da Costa, T. Melo, E. Maciel, A. Rego, M.H. Abreu, P. Domingues, and R. Calado. 2019. Lipidomic signature of the green macroalgae Ulva rigida farmed in a sustainable integrated multi-trophic aquaculture. *Journal of Applied Phycology*. 31:1369-1381.

Loughnane, C.J., L.M. McIvor, F. Rindi, D.B. Stengel, and M.D. Guiry. 2008. Morphology, rbcL phylogeny and distribution of distromatic Ulva (Ulvophyceae, Chlorophyta) in Ireland and southern Britain. *Phycologia*. 47:416-429.

Lüning, K., and M. Dring. 1975. Reproduction, growth and photosynthesis of gametophytes of Laminaria saccharina grown in blue and red light. *Mar Biol*. 29:195-200.

Luttikhuizen, P.C., F.H. van den Heuvel, C. Rebours, H.J. Witte, J.D. van Bleijswijk, and K. Timmermans. 2018. Strong population structure but no equilibrium yet: Genetic connectivity and phylogeography in the kelp Saccharina latissima (Laminariales, Phaeophyta). *Ecology and evolution*. 8:4265-4277.

Magnusson, M., C.R. Glasson, M.J. Vucko, A. Angell, T.L. Neoh, and R. de Nys. 2019. Enrichment processes for the production of high-protein feed from the green seaweed Ulva ohnoi. *Algal Research*. 41:101555.

Mariotti, F., D. Tomé, and P.P. Mirand. 2008. Converting nitrogen into protein—beyond 6.25 and Jones' factors. *Critical reviews in food science and nutrition*. 48:177-184.

Moller Nielsen, M., C. Paulino, J. Neiva, D. Krause-Jensen, A. Bruhn, and E.A. Serrao. 2016. Genetic diversity of Saccharina latissima (Phaeophyceae) along a salinity gradient in the North Sea-Baltic Sea transition zone. *J Phycol*. 52:523-531.

Mooney, K.M., G.E. Beatty, B. Elsasser, E.S. Follis, L. Kregting, N.E. O'Connor, G.E. Riddell, and J. Provan. 2018. Hierarchical structuring of genetic variation at differing geographic scales in the cultivated sugar kelp Saccharina latissima. *Mar Environ Res*. 142:108-115.

Murua, P. in prep. Disease resistance strategies across Phaeophyceae are multi-layered and conserved mechanisms against phylogenetically unrelated pathogens.

Neiva, J., C. Paulino, M.M. Nielsen, D. Krause-Jensen, G.W. Saunders, J. Assis, I. Barbara, E. Tamigneaux, L. Gouveia, T. Aires, N. Marba, A. Bruhn, G.A. Pearson, and E.A. Serrao. 2018. Glacial vicariance drives phylogeographic diversification in the amphi-boreal kelp Saccharina latissima. *Sci Rep*. 8:1112.

Paulino, C., J. Neiva, N.C. Coelho, T. Aires, N. Marbà, D. Krause-Jensen, and E.A. Serrão. 2016. Characterization of 12 polymorphic microsatellite markers in the sugar kelp Saccharina latissima. *J Appl Phycol*. 28:3071-3074.

Robertson-Andersson, D., D. Wilson, J.J. Bolton, R.J. Anderson, and G. Maneveldt. 2009. Rapid assessment of tissue nitrogen in cultivated Gracilaria gracilis (Rhodophyta) and Ulva lactuca (Chlorophyta). *African Journal of Aquatic Science*. 34:169-172.

Rueden, C.T., J. Schindelin, M.C. Hiner, B.E. DeZonia, A.E. Walter, E.T. Arena, and K.W. Eliceiri. 2017. ImageJ2: ImageJ for the next generation of scientific image data. *BMC Bioinformatics*. 18:529.

Shpigel, M., L. Guttman, L. Shauli, V. Odintsov, D. Ben-Ezra, and S. Harpaz. 2017. Ulva lactuca from an Integrated Multi-Trophic Aquaculture (IMTA) biofilter system as a protein supplement in gilthead seabream (Sparus aurata) diet. *Aquaculture*. 481:112-118.

Silva, D.M., L.M.P. Valente, I. Sousa-Pinto, R. Pereira, M.A. Pires, F. Seixas, and P. Rema. 2015. Evaluation of IMTA-produced seaweeds (Gracilaria, Porphyra, and Ulva) as dietary ingredients

in Nile tilapia, Oreochromis niloticus L., juveniles. Effects on growth performance and gut histology. *Journal of Applied Phycology*. 27:1671-1680.

Steinhagen, S., A. Barco, T. Wichard, and F. Weinberger. 2019. Conspecificity of the model organism Ulva mutabilis and Ulva compressa (Ulvophyceae, Chlorophyta). *Journal of phycology*. 55:25-36.

Visch, W., C. Rad-Menendez, G.M. Nylund, H. Pavia, M.J. Ryan, and J. Day. 2019. Underpinning the Development of Seaweed Biotechnology: Cryopreservation of Brown Algae (Saccharina latissima) Gametophytes. *Biopreserv Biobank*. 17:378-386.

Wang, X., Z. Chen, Q. Li, J. Zhang, S. Liu, and D. Duan. 2018. High-density SNP-based QTL mapping and candidate gene screening for yield-related blade length and width in Saccharina japonica (Laminariales, Phaeophyta). *Sci Rep*. 8:13591.

Wichard, T. 2015. Exploring bacteria-induced growth and morphogenesis in the green macroalga order Ulvales (Chlorophyta). *Front Plant Sci*. 6:86.

Xiao, Y., H. Liu, L. Wu, M. Warburton, and J. Yan. 2017. Genome-wide Association Studies in Maize: Praise and Stargaze. *Mol Plant*. 10:359-374.

Zhang, J., T. Liu, R. Feng, C. Liu, and S. Chi. 2015. Genetic Map Construction and Quantitative Trait Locus (QTL) Detection of Six Economic Traits Using an F2 Population of the Hybrid from Saccharina longissima and Saccharina japonica. *PLoS One*. 10:e0128588.